

# Archosauriform footprints in the Lower Triassic of Western Alps and their role in understanding the effects of the Permian-Triassic hyperthermal (#51782)

1

First submission

## Guidance from your Editor

Please submit by **27 Aug 2020** for the benefit of the authors (and your \$200 publishing discount) .



### Structure and Criteria

Please read the 'Structure and Criteria' page for general guidance.



### Custom checks

Make sure you include the custom checks shown below, in your review.



### Raw data check

Review the raw data.



### Image check

Check that figures and images have not been inappropriately manipulated.

Privacy reminder: If uploading an annotated PDF, remove identifiable information to remain anonymous.

## Files

Download and review all files from the [materials page](#).

11 Figure file(s)

1 Video file(s)

## Custom checks

### New species checks



Have you checked our [new species policies](#)?



Do you agree that it is a new species?



Is it correctly described e.g. meets ICZN standard?



## Structure your review

The review form is divided into 5 sections. Please consider these when composing your review:

- 1. BASIC REPORTING**
- 2. EXPERIMENTAL DESIGN**
- 3. VALIDITY OF THE FINDINGS**

4. General comments
5. Confidential notes to the editor

You can also annotate this PDF and upload it as part of your review

When ready [submit online](#).

## Editorial Criteria

Use these criteria points to structure your review. The full detailed editorial criteria is on your [guidance page](#).

### BASIC REPORTING

- Clear, unambiguous, professional English language used throughout.
- Intro & background to show context. Literature well referenced & relevant.
- Structure conforms to [PeerJ standards](#), discipline norm, or improved for clarity.
- Figures are relevant, high quality, well labelled & described.
- Raw data supplied (see [PeerJ policy](#)).

### EXPERIMENTAL DESIGN

- Original primary research within [Scope of the journal](#).
- Research question well defined, relevant & meaningful. It is stated how the research fills an identified knowledge gap.
- Rigorous investigation performed to a high technical & ethical standard.
- Methods described with sufficient detail & information to replicate.

### VALIDITY OF THE FINDINGS

- Impact and novelty not assessed. Negative/inconclusive results accepted. *Meaningful* replication encouraged where rationale & benefit to literature is clearly stated.
- All underlying data have been provided; they are robust, statistically sound, & controlled.

- Speculation is welcome, but should be identified as such.
- Conclusions are well stated, linked to original research question & limited to supporting results.

# Standout reviewing tips

3



The best reviewers use these techniques

## Tip

**Support criticisms with evidence from the text or from other sources**

**Give specific suggestions on how to improve the manuscript**

**Comment on language and grammar issues**

**Organize by importance of the issues, and number your points**

**Please provide constructive criticism, and avoid personal opinions**

**Comment on strengths (as well as weaknesses) of the manuscript**

## Example

*Smith et al (J of Methodology, 2005, V3, pp 123) have shown that the analysis you use in Lines 241-250 is not the most appropriate for this situation. Please explain why you used this method.*

*Your introduction needs more detail. I suggest that you improve the description at lines 57- 86 to provide more justification for your study (specifically, you should expand upon the knowledge gap being filled).*

*The English language should be improved to ensure that an international audience can clearly understand your text. Some examples where the language could be improved include lines 23, 77, 121, 128 - the current phrasing makes comprehension difficult.*

1. Your most important issue
2. The next most important item
3. ...
4. The least important points

*I thank you for providing the raw data, however your supplemental files need more descriptive metadata identifiers to be useful to future readers. Although your results are compelling, the data analysis should be improved in the following ways: AA, BB, CC*

*I commend the authors for their extensive data set, compiled over many years of detailed fieldwork. In addition, the manuscript is clearly written in professional, unambiguous language. If there is a weakness, it is in the statistical analysis (as I have noted above) which should be improved upon before Acceptance.*

# Archosauriform footprints in the Lower Triassic of Western Alps and their role in understanding the effects of the Permian-Triassic hyperthermal

Fabio M. Petti <sup>1</sup>, Heinz Furrer <sup>2</sup>, Enrico Collo <sup>3</sup>, Edoardo Martinetto <sup>4</sup>, Massimo Bernardi <sup>1</sup>, Massimo Delfino <sup>4</sup>, Marco Romano <sup>Corresp. 5</sup>, Michele Piazza <sup>6</sup>

<sup>1</sup> MUSE – Museo delle Scienze, Trento, Trento, Italy

<sup>2</sup> Paläontologisches Institut und Museum, Universität Zürich, Zürich, Switzerland

<sup>3</sup> Natura Occitana, Dronero (CN), Dronero (CN), Italy

<sup>4</sup> Dipartimento di Scienze della Terra, Università degli Studi di Torino, Torin, Italy

<sup>5</sup> Scienze della Terra, University of Roma "La Sapienza", Rome, Italy

<sup>6</sup> Dipartimento di Scienze della Terra, dell'Ambiente e della Vita, Università di Genova, Genoa, Italy

Corresponding Author: Marco Romano  
Email address: marco.romano@uniroma1.it

The most accepted killing model for the Permian-Triassic mass extinction (PTME) postulates that massive volcanic eruption (i.e. the Siberian Traps LIP) led to geologically rapid global warming, acid rain and ocean anoxia. On land, habitable zones were drastically reduced, due to the combined effects of heating, drought and acid rains. This hyperthermal had severe effects also on the paleobiogeography of several groups of organisms. Among those, the tetrapods, whose geographical distribution across the end-Permian mass extinction (EPME) was the subject of controversy of a number of recent papers. We here describe and interpret a new Early Triassic (?Olenekian) archosaur track assemblage from the Gardetta Plateau (Briançonnais, Western Alps, Italy) which, at the Permian-Triassic boundary, was placed at about 11° North. The tracks, both arranged in trackways and documented by single, well-preserved imprints, are assigned to *Isochirotherium gardettae* ichnosp. nov., and are here interpreted as produced by a non-archosaurian archosauriform (erytrosuchid?) trackmaker. This new discovery provides further evidence for the presence of archosauriformes at low latitudes during the Early Triassic epoch, supporting a model in which the PTME did not completely vacate low-latitude lands from tetrapods that therefore would have been able to cope with the extreme hot temperatures of Pangaea mainland.

# 1 Archosauriform footprints in the Lower Triassic of Western Alps and their 2 role in understanding the effects of the Permian-Triassic hyperthermal

3

4 Fabio M. Petti<sup>1</sup>, Heinz Furrer<sup>2</sup>, Enrico Collo<sup>3</sup>,

5 Edoardo Martinetto<sup>4</sup>, Massimo Bernardi<sup>1</sup>, Massimo Delfino<sup>4</sup>, Marco Romano<sup>5,\*</sup>

6 and Michele Piazza<sup>6</sup>

7

8 <sup>1</sup>MUSE – Museo delle Scienze, Trento

9 <sup>2</sup>Paläontologisches Institut und Museum, Universität Zürich, Zürich

## 10 <sup>3</sup>Natura Occitana, Dronero (CN)

11 <sup>4</sup>Dipartimento di Scienze della Terra, Università degli Studi di Torino, Torino

12 <sup>5</sup>Dipartimento di Scienze della Terra, Sapienza Università di Roma, Roma

13 <sup>6</sup>Dipartimento di Scienze della Terra, dell'Ambiente e della Vita, Università di Genova, Genova

14

15 \*Corresponding author e-mail: marco.romano@uniroma1.it

16

17 *Key words: Isochirotherium gardettae* n. ichnosp., climate warming, extinction, Lower Triassic,

18 Italy.

19

20

21

22

23

## 24 ABSTRACT

25 The most accepted killing model for the Permian-Triassic mass extinction (PTME) postulates  
26 that massive volcanic eruption (i.e. the Siberian Traps LIP) led to geologically rapid global  
27 warming, acid rain and ocean anoxia. On land, habitable zones were drastically reduced, due to  
28 the combined effects of heating, drought and acid rains. This hyperthermal had severe effects  
29 also on the paleobiogeography of several groups of organisms. Among those, the tetrapods,  
30 whose geographical distribution across the end-Permian mass extinction (EPME) was the subject  
31 of controversy of a number of recent papers. We here describe and interpret a new Early Triassic  
32 (?Olenekian) archosaur track assemblage from the Gardetta Plateau (Briançonnais, Western  
33 Alps, Italy) which, at the Permian-Triassic boundary, was placed at about 11° North. The tracks,  
34 both arranged in trackways and documented by single, well-preserved imprints, are assigned to  
35 *Isochirotherium gardettae* ichnosp. nov., and are here interpreted as produced by a non-  
36 archosaurian archosauriform (erythrosuchid?) trackmaker. This new discovery provides further  
37 evidence for the presence of archosauriformes at low latitudes during the Early Triassic epoch,  
38 supporting a model in which the PTME did not completely vacate low-latitude lands from  
39 tetrapods that therefore would have been able to cope with the extreme hot temperatures of  
40 Pangaea mainland.

41

42

## 43 INTRODUCTION

44

45 The Permian-Triassic mass extinction (PTME) was the most severe biotic crisis of all times  
46 (Erwin, 1993), eliminating > 90% of marine and terrestrial species (Erwin, 1993; Song et al.,  
47 2013, 2015). After the mass extinction, totally new clades emerged, which include decapods and  
48 marine reptiles in the oceans and new tetrapods on land (Chen and Benton, 2012). In the last  
49 decade different physical environmental shocks have been identified as possible triggers for the  
50 huge crisis, which include increased atmospheric CO<sub>2</sub> concentrations, global warming, acid rain,  
51 ocean anoxia, ocean acidification and hypercapnia (Chen and Benton, 2012; Benton, 2018). The  
52 most accepted killing model (e.g. Benton & Twitchett, 2003; Chen & Benton, 2012; Benton &  
53 Newell, 2014; Shen et al., 2019) postulates an initial megascale eruption (more than 1,000  
54 Gigatonnes of erupted lava, see Grasby et al., 2011), that released **consistent amount** of sulphate  
55 aerosols and methane from clathrate reservoirs (see Berner, 2002), which led to global warming  
56 and acid rain, causing a generalized plant die-offs and thus intensive erosion of the soil (Wignall,  
57 2001; Benton, 2003, 2018; Benton & Twitchett, 2003; Sephton et al., 2005; Knoll et al., 2007).  
58 On land, habitable zones were drastically reduced, due to the combination of extreme heat,  
59 drought and acid rains, which caused progressive loss of soil and forests and had direct impact  
60 on lacustrine organisms and any land-dwelling animal (Benton & Newell, 2014).

61 According to several authors (Joachimski et al., 2012; Sun et al., 2012; Schobben et al., 2014;  
62 Song et al., 2015) the intense global warming started at the extinction horizon as testified in the  
63 Meishan section (South China), and then continued in the Early Triassic, very likely with the  
64 release of methane from deep ocean sediments and coals that triggered the process, and the  
65 release of additional greenhouse gasses by interactions of the Siberian traps with local  
66 permafrost soils, limestones, and other deposits rich in organic matter (e.g. Racki, 2003; Racki &  
67 Wignall, 2005; Retallack & Jahren, 2008; Grasby et al., 2011).



68 The hyperthermal had severe effects also on the paleobiogeographic patterns. In ~~the last~~ years  
69 the distribution of land tetrapods across the PTME was discussed ~~by~~ a number of studies which  
70 however suggested different scenarios. By compiling literature evidence on the main skeletal  
71 findings, Sun et al. (2012) suggested that, in the Early Triassic, terrestrial vertebrates totally  
72 vacated the equatorial belt, the so-called 'vertebrate equatorial-gap', as a consequence of the  
73 extreme hot temperatures. More recently, Bernardi et al. (2015, 2018) reviewed the Late  
74 Permian-Early Triassic terrestrial tetrapod record integrating skeletal and track data and  
75 concluded that tetrapod geographic distribution was much wider than previously suggested. In  
76 the Early Triassic it included also the low latitudes, though polarward dispersals were detected in  
77 the Early Triassic and possibly linked to the development of super-hot temperatures in the  
78 equatorial belt (Bernardi et al., 2018). Fossil track evidence, in particular, was key in denying the  
79 existence of an 'equatorial gap' (Bernardi et al., 2018).

80 Archosaur tracks and trackways are in fact well-known from Lower to Middle Triassic  
81 siliciclastic and carbonate sediments of the Upper Buntsandstein and Lower Muschelkalk (late  
82 Olenekian-early Anisian) of Germany (Haubold, 1971a, 1971b; Klein & Haubold, 2007), the  
83 Lower Triassic of the Holy Cross Mountains in Poland (Klein & Niedzwiedski, 2012), the  
84 Middle Triassic of Bourgogne (Gand, 1979), Massif Central (Demathieu, 1970) and Ardèche in  
85 France (Courel & Demathieu, 1976), the Iberian Range in Spain (Fortuny et al., 2011; Diaz-  
86 Martinez, et al., 2015) and Sardinia in Italy (Citton et al., 2020). Further sites, often with  
87 identical ichnotaxa and ichnoassemblages, are known from the Lower to Middle Triassic of  
88 Great Britain (King et al., 2005), North American southwest (Klein & Lucas, 2010), Argentina  
89 (Melchor & De Valais, 2006), Africa (Klein et al., 2011) and southern China (Xing et al., 2013).  
90 In the Alps, chirotherian footprints were described from the Lower to Middle Triassic of the

91 Dolomites, Piedmont and Ligurian Alps in Italy (Avanzini & Mietto, 2008; Petti et al., 2013;  
92 Santi et al., 2015), Aar Massif in eastern Switzerland (Feldmann et al., 2009; Klein et al., 2016)  
93 and the Aiguilles Rouges Massif (Western Alps), on the border between Switzerland and France  
94 (Demathieu & Weidmann, 1982; Avanzini & Cavin, 2009; Cavin et al., 2012; Klein et al., 2016).

95 We here describe and interpret a new archosaur track assemblage from the Gardetta Plateau  
96 (Western Alps, south-western Piedmont, Italy; Fig. 1) that was analyzed in two different field  
97 ~~works~~ during the summer 2009 and in the autumn 2017-2018.

98 Tracks are preserved on two distinct track surfaces, belonging to the same stratigraphic  
99 horizon. Some of them are badly preserved but distinct trackways, up to 3 m long, can be  
100 recognized together with other exceptionally preserved isolated tracks showing clear  
101 morphological details of the trackmaker's autopodium.

102 This discovery provides reliable evidence of the presence of archosauriforms in the  
103 Briançonnais domain during the Early Triassic, adding further support to the occurrence of  
104 terrestrial tetrapods at low latitudes soon after the PTME (Bernardi et al., 2015; 2018) and well-  
105 before a full land ecosystem recovery.

106

107

## 108 MATERIALS AND METHODS

109

110 All the specimens were identified in the same outcrop, located about 1 km SE of the Gardetta  
111 Plateau, close to Pianezza creek (44°24'5.75"N; 7° 1'45.29"E; Canosio Municipality, Cuneo  
112 Province, NW Italy; Fig. 1).

113 Most of the footprints are preserved as negative epichnia (concave epirelief) and were left *in*  
114 *situ* in the field. The footprints were discovered by EC and MP in summer 2008. A surface of  
115 about 10-15 m<sup>2</sup> was mapped ~~a~~ first time in 2009 by HF and then in 2017 by FP and HF. An  
116 exceptionally preserved trackway, consisting of three large pes and manus imprints, was then  
117 discovered during the 2017 and 2018 field ~~works~~ by EM and FP, about 10 m higher up on the  
118 same outcropping horizon. Tracks outlines were drawn on transparency acetate film and then  
119 digitized by a vector-based drawing software (Adobe Illustrator ©). Additional footprints were  
120 collected by the authors and hikers from loose sandstone slabs in the creek below the track  
121 surfaces. These isolated and usually fragmentary footprints are preserved both as concave  
122 epirelief and well-preserved convex epirelief, the latter being preserved in the basalmost level of  
123 the sandstone bed which overlies the track layer.

124 Close-range photogrammetry was used to document tracks and obtain three-dimensional  
125 model of the best-preserved ones (Petti et al., 2008; Remondino et al., 2010; Mallison & Wings,  
126 2014). The data processing phase was performed using Agisoft PhotoScan ® Professional  
127 software, following the procedure indicated by Mallison & Wings (2014). In a second phase, the  
128 software Surfer®14 (GoldenSoftware, 2002), was used to convert elevation points to contour  
129 lines and to produce color coded maps of the studied material.

130 The obtained images are ideal for both ~~precisely measure~~ standard ichological parameters  
131 (Haubold, 1971b; Leonardi, 1987) and for recognizing anatomy related morphologies, therefore  
132 for the reconstruction of the trackmaker's autopodial osteology.

133 **Trackmaker identification** was carried out employing three different and integrated  
134 methodological approaches: i) Synapomorphy-based correlation (Olsen, 1995; Carrano &  
135 Wilson, 2001); ii) Phenetic correlation (Carrano & Wilson, 2001) and iii) Coincidence

136 correlation (Carrano & Wilson, 2001). The synapomorphy-based method focuses on the  
137 identification of osteologic-derived character states in the footprints that result from the  
138 impression of synapomorphic characters in the trackmaker autopodia (see Olsen et al., 1998;  
139 Carrano & Wilson, 2001; Wilson, 2005; Romano et al., 2015). The phenetic correlation is  
140 closely linked to ichnotaxonomy and derives from an accurate description of the footprint and  
141 the identification of the trackmaker through the recognition of an affinity between tracks and  
142 limbs osteology (Carrano & Wilson, 2001; Wilson, 2005). The coincidence correlation is usually  
143 adopted to refine trackmaker identification and is based on supplemental data including  
144 geological age, geographic provenance, local faunal composition and distributions, and  
145 abundances of skeletal taxa and ichnotaxa (Carrano & Wilson, 2001).

146

147

## 148 GEOLOGICAL FRAMEWORK

149

150 The Gardetta Plateau - Preit valley area is located in the southern part of the Western Alps  
151 (Fig. 1). It encompasses the Sautron, Rouchouze, Rocca Peroni tectonic units and the Gardetta  
152 deformation unit (*sensu* d'Atri et al., 2016) also known as “bande siliceuse de la Gardetta”  
153 (Gidon, 1972). These tectonic units pertain to the Briançonnais Domain (Gidon, 1958a, 1958b,  
154 1972; Schmid et al., 2004, 2017) and in particular to the External Briançonnais Domain which is  
155 characterized by very low grade to anchizone metamorphism (d'Atri et al., 2016).

156 The upper Permian-Mesozoic sedimentary succession varies considerably within the

157 Briançonnais Domain *s.l.* (Briançonnais Domain *s.s.* and Ligurian Briançonnais, Decarlis &  
158 Lualdi, 2009; Fig. 2) due to the slightly different paleogeographic positions of these sectors (see

159 Decarlis et al., 2013 for a review). The outcropping lithostratigraphic units, even if can be  
160 correlated across the distinct domains, display different thickness, vertical/lateral relationships  
161 and hiatuses. These differences led authors to adopt a multitude of official and unofficial names  
162 for the lithostratigraphic units. Despite these minor differences, the late Permian–Early Triassic  
163 sedimentation in the whole Briançonnais domain s.l. testifies to the evolution of a continental  
164 margin affected by extensional tectonics. The Briançonnais domain was positioned north of the  
165 westernmost sector of the Palaeotethys, in the western continental termination of the Meliata  
166 oceanic back-arc basin (Ziegler & Stampfli, 2001; Decarlis et al., 2013). Adopting the  
167 paleolatitude calculator developed by Van Hinsbergen et al. (2015) (model version 2.1) and  
168 using the Global Apparent Polar Wander Path of Torsvik et al. (2012) as paleomagnetic  
169 reference frame, the Early Triassic (250 Ma) palaeolatitude estimate for the Southern  
170 Briançonnais Domain is 11.8 N.

171 In the study area the volcano-sedimentary succession starts with upper Carboniferous -  
172 Permian volcanic rocks (andesitic lavas followed by rhyolites and rhyolitic ignimbrites)  
173 unconformably overlain by upper Permian-Lower Triassic siliciclastic continental-to-transitional  
174 deposits (the so called “*semelle silicieuse*” of French Authors). In particular these deposits are  
175 characterized by basal coarse grained conglomerates and quartz-conglomerates, named locally  
176 “Verrucano Brianzonese”, (Carraro et al., 1970; Cassinis et al., 2018) that evolve upward into  
177 quartz-arenites and quartz-siltites of the “Werfenian quartzites” (Fig. 2; Gidon, 1958b; Malaroda,  
178 1970; Megard-Galli & Baud, 1977; Costamagna et al., 2002; Costamagna, 2013). The  
179 siliciclastic sequence indicate deposition in an alluvial environment characterized by sandy  
180 braided fluvial system fed by the residual Variscan relieves (Costamagna, 2013). In the  
181 southernmost part of the Briançonnais domain (External Ligurian Briançonnais Domain,

182 Vanossi, 1974; 1991; Bertok et al., 2012) these latter lithostratigraphic units are known as  
183 “Scytian quartzites” or “Ponte di Nava Quarzites” (Fig. 2; Decarlis et al., 2013, 2015). Similar to  
184 the siliciclastic sequence of the Briançonnais Domain s.s., the “Ponte di Nava Quarzites”  
185 originated from the dismantling and reworking of the Paleozoic igneous and metamorphic  
186 basement.

187 The quartz-arenites can be topped either by greenish pelites (known as “Case Valmarenca  
188 Pelites” in the Ligurian Briançonnais, Vanossi 1974; 1991), that have been interpreted as mudflat  
189 deposits, or by a thin and discontinuous interval of cavernous dolostones called “*Cargneules*  
190 *Inférieures*” representing the sedimentation in an arid environment as an evaporitic sabkha (Fig.  
191 2). According to Lualdi & Seno (1984), in the Ligurian Briançonnais Zone the “Case  
192 Valmarenca Pelites” could be laterally equivalent to the “*Cargneules inférieures*”.

193 The continental succession and/or the evaporitic deposits are followed by Middle Triassic  
194 shallow water carbonates of the “*couverture carbonatée*” (Gidon, 1958b; Megard-Galli & Baud,  
195 1977; Costamagna et al., 2002) comprising a lower calcareous complex (Costa Losera Fm,  
196 Lualdi and Bianchi, 1990, corresponding to the e St. Triphon Formation of the classic  
197 Briançonnais Domain) and an upper dolomitic complex (San Pietro dei Monti Fm, Vanossi,  
198 1969). These carbonate deposits testify the sedimentation in a subsiding carbonate ramp.

199 The lower calcareous complex (Fig. 2) begins with a characteristic facies named “*Marbres*  
200 *Phylliteux*” by French Authors made of greyish and brownish fine-grained limestones, (lower to  
201 upper Anisian) with sericite, muscovite, chlorite laminated levels. Bedding can be locally  
202 masked by pervasive and intense bioturbation (“*Calcaires Vermiculés*” facies) assigned to the  
203 ichnogenus *Rhizocorallium*. The basal complex ends with varicolored pelites, interpreted as

204 cinerites (upper Anisian in age) by Caby & Galli (1964), recognizable throughout the whole  
205 Briançonnais Domain.

206 The upper dolomitic complex (Fig. 2) is ~~constituted by~~ massive to well-bedded dolostones  
207 followed by cyclically arranged carbonates (“*Calcaires rubanés*” – upper Anisian – upper  
208 Ladinian; Gidon, 1958b; Megard-Galli & Baud, 1977; Costamagna et al., 2002; Decarlis &  
209 Lualdi, 2009) characterized by subtidal crinoidal wackestones, intertidal oolitic limestones and  
210 supratidal dolomitic mudstones capped by reddish paleosols, that testify shallowing-upward  
211 cycles. The dolomitic succession includes dark limestones, dark fossiliferous and/or oolithic  
212 dolostones, meter-thick autoclastic breccias and gypsum–anhydrite pseudomorphs witnesses of  
213 major emersion events. These lithofacies, dated to the uppermost Ladinian, are known in the  
214 different Briançonnais domains as “*Dolomies blanches*” or “*Dolomies grises*” or “Couches a C.  
215 *goldfussi*” or “*Complexe schisto-dolomitique basal*”.

216

217

## 218 THE PIAНЕZZА STRATIGRAPHIC SUCCESSION

219

220 In the framework of the abovementioned stratigraphic setting the footprint-bearing level is  
221 located in the Pianezza area along the track connecting Colle del Preit (2100 m a.s.l.) to Grange  
222 Isoardi (Pianezza area, 2275 m a.s.l.) (Fig. 2). The outcrop is located along the SW flank of a  
223 narrow antiformal anticline belonging to the Sautron Tectonic Unit which overthrusts the  
224 Rouchouze Tectonic Unit. Here the volcano-stratigraphic succession begins by meta-andesites  
225 and andesitic schists pertaining to the upper Carboniferous-Permian volcanic complex. The  
226 sedimentary succession continues upward with a thin and discontinuous (up to 1 meter) level of

227 graphitic schists, deriving from the weathering of the volcanic basement (Lorenzoni & Zanettin,  
228 1958) and is then followed by up to 100 meters of quartz-conglomerates (“Verrucano  
229 Brianzese”) and by fine to very fine quartz-arenite and quartz-siltite with ripple marks and  
230 cross bedding (“Werfenian quartzites”). The track-bearing horizon occurs at the top of the latter  
231 clastic interval. The succession continues upward with 15 meters of gypsum/anhydrite deposits  
232 of the lower cargneule. In the Pianezza area the Middle Triassic “couverture carbonatée” is only  
233 represented in the north-eastern flank of Sautron Unit anticline.

234

235

## 236 CHRONOSTRATIGRAPHIC FRAMEWORK OF THE STUDY AREA

237

238 The sedimentary rocks belonging to the quartz-rich clastic succession does not allow precise  
239 dating because of the lack of biostratigraphic markers as commonly happen for these kind of  
240 deposits. They are here referred to the upper Permian-Lower Triassic on the base of their  
241 stratigraphic position in the Sautron Unit, similar to that of the well-comparable quartz-  
242 conglomerate and quartzarenite rocks occurring not only in the Briançonnais Domain, but also in  
243 the Southern Alps, Sardinia and Provence. For this reason, in order to constrain the age of the  
244 track-bearing horizon, some considerations are required: i) the coarse quartz-conglomerates  
245 (“Verrucano Brianzese”) are commonly referred to the late Permian-earliest Triassic (Gidon,  
246 1958b; Carraro et al., 1970; Megard-Galli & Baud, 1977; Decarlis & Lualdi, 2009); ii) the Lower  
247 Triassic age can be hypothesized considering the occurrence of *Estheria minuta* Alberti and  
248 *Myacites fassaensis* Bittner within the “Ponte di Nava Quarzites” (Decarlis & Lualdi, 2009); iii)  
249 the “lower cargneule” unit and its lateral equivalent “Case Val Marenca Pelites” are generally

250 attributed to the late Early Triassic (Gidon, 1958b; Carraro et al., 1970; Megard-Galli & Baud,  
251 1977; Decarlis & Lualdi, 2009); iv) the lower part of “*Marbres Phylliteux*” are considered early  
252 Anisian in age, on the basis of the occurrence of *Rhizocorallium*, that is regarded to be an early  
253 Anisian marker all over the Tethyan realm (Baud, 1976); v) an early Anisian age for the base of  
254 the lower calcareous complex (“*Marbres Phylliteux*” and Costa Losera Fm.) is also suggested by  
255 the occurrence of Dasycladacean algae and crinoidal remains (*Dadocrinus* sp.; Carraro et al.,  
256 1970); vi) In the northern Briançonnais of southwestern Switzerland a find of the ammonoid  
257 *Beyrichites cadoricus* in the upper part of the St-Triphon Formation indicate a middle Anisian  
258 age (Baud et al., 2016).

259 Additionally, it is worth mentioning that both in the Geological Map of the Argentera Massif  
260 (Malaroda, 1970; Carraro et al., 1970) and in the Geological Map of France at the scale 1: 50.000  
261 (Sheet 896, Larche; Gidon, 1978) the studied outcrop was attributed to Lower Triassic. All the  
262 above reported data thus point to a probable attribution of the trampled horizon to the late Early  
263 Triassic.

264

265

## 266 SYSTEMATIC ICHNOLOGY

267

268 Most footprints are preserved as natural molds (concave epirelief) on top of a 3-4 cm thick  
269 bed of fine sandstone. The tracks are shallow, less than 2 cm deep, but most of them are cut by  
270 small-scale tectonic cracks/fissures and strongly weathered. Two possible trackways with lengths  
271 of 4–5 m were identified on a track surface. Only one isolated track was visible on the  
272 underlying sandstone bed, also preserved as concave epirelief. Three solitary small footprints,

273 preserved as convex epirelief of the directly overlying sandstone bed, were collected from loose  
274 slabs. The upper surface of this 1–2 cm thick sandstone bed is marked by symmetric wave  
275 ripples, exposed on a spectacular bedding plane (Fig. 3).

276 An exceptionally preserved trackway, made of three consecutive manus-pes sets was found on  
277 another surface, belonging to the same stratigraphic horizon, upstream of the previously  
278 described ones (Fig. 4). The general features of the herein studied ichnoassemblage are typical  
279 for chirotherian tracks (Haubold & Klein, 2002).

280

281

282 **Ichnogenus *Chirotherium* Kaup, 1835**

283 **Type ichnospecies:** *Chirotherium barthii* Kaup, 1835

284

285 *Chirotherium* isp.

286 (Figs 3, 7)

287 **Referred specimens:** two trackways preserved as concave epirelief (GT-1 and GT-2). GT-1  
288 consists of four clear and two weakly impressed imprints, arranged in a 2.10 m-long trackway in  
289 the lower part of the outcrop, just 2 meters above the creek level (Fig. 3). Its direction on the  
290 steep bedding plane points upwards to southeast. Trackway GT-2 is 2.40-m-long, is preserved in  
291 the lower part of the same bedding plane, about 2 meters above the creek level, running from  
292 northwest to southeast.

293

294 **Description:** pentadactyl and semi-digitigrade pes imprint. Pes is longer than wide, (Foot  
295 Length [FL] = 13 to 16 cm; Foot Width [FW] = 8-10 cm; FL/FW = 1.6 to 2.0) with digit group

296 II-IV roughly asymmetrical. Pedal digit impressions gradually increase from I to IV, with II sub-  
297 equal or shorter than digit IV; digit III is the longest. In the best-preserved track (GT1-3; Figs 3,  
298 7), digit I is pointed and placed posteriorly with respect to digit group II-IV. Digit V is oval and  
299 tapers distally; it is positioned posteriorly and laterally to digit I-IV and directed antero-laterally.  
300 No digital pad impressions can be observed on digit II-IV. Digit V shows a large rounded pad  
301 impression and a possible sub-triangular shaped claw mark. Manus tracks are absent or faintly  
302 preserved as small semi-circular imprints, placed in front of the pedal footprints. An isolated  
303 tetradactyl imprints, measuring 4.5 cm in length and 7 cm in width, and another isolated circular  
304 pentadactyl imprint 5.5 cm long are interpreted as possible manus imprints.

305 In the trackway the oblique pace varies between 26 and 41 cm, with a mean value of 36 cm.  
306 The pes pace angulation varies between 145° and 165°, with a mean value of 157°.

307

308 **Discussion:** the ichnogenus *Chirotherium* with its holotype *Chirotherium barthii*, was  
309 described by Kaup (1835) on trackways from the “Thüringischer Chirotheriensandstein” (Lower-  
310 Middle Triassic) of the Thuringia region (Germany). The here described material, even if not  
311 perfectly preserved, retains some diagnostic features of the ichnogenus *Chirotherium*, such as the  
312 oval morphology and the position of digit V (slightly behind digit group II-IV), and the relative  
313 digit length of group II-IV, with digit IV longer or sub-equal to digit II. Pes pace angulation is  
314 also similar to the values to date reported for the ichnogenus (160°-170°). *Chirotherium barthii*  
315 (Figs 7e, 7f) shows clear circular pads on digit group II-IV and digit impressions are broader  
316 than in the studied specimens. In *C. barthii*, as well as in *C. rex*, *C. moquinense* and *C. vorbachi*  
317 (Fig. 7h), digits I-IV are splayed whereas in the GT-1 and GT-2 trackways, pedal digits outlines  
318 are closely arranged with only digit I medially spread. Digits II-IV seems to be almost parallel to

319 each other and the digit pattern resemble that of the ichnospecies *C. sickleri* Kaup, 1835 (Figs 7i,  
320 7l, 7m) with digit I forming a narrow group with digits II, III and IV. Nevertheless, digit IV,  
321 though slightly shorter than III, is not much longer than II as observed in most of the specimens  
322 assigned to *C. sickleri*. Unfortunately, the bad preservation of pes imprints in GT-1 and GT-2  
323 trackways preclude any accurate ichnospecific assignment.

324

325 **Ichnogenus *Isochirotherium* Haubold, 1971a** (Figs 4, 5, 8)

326 **Type ichnospesies: *Isochirotherium soergeli* (Haubold, 1967).**

327

328 ***Isochirotherium gardettae* ichnosp. nov.**

329

330 **Derivatio nominis:** from the Gardetta plateau, type locality of the ichnospecies.

331

332 **Type-level:** “Werfenian quartzites”, Lower Triassic.

333

334 **Referred specimens:** a trackway made of three well-preserved and consecutive manus-pes  
335 couples (GT-7; Fig. 4) not exceeding 2.20 m across. Another possible isolated track (GT-3)  
336 partially preserved in the lower track surface.

337

338 **Diagnosis:** chirotherian track with pentadactyl pes and small and tetradactyl manus imprint  
339 and pes digit IV noticeably shorter than II; pes digit group I-IV slightly longer than wide, pes  
340 digit V with large ovoid metatarsal pad and a reduced phalangeal portion. Pes length ranging

341 from 28 to 33 cm; cross axis equal to 90°. Trackway very narrow, pace angulation near 165°, and  
342 ratio of stride to pes length is 4.3.

343

344 **Description:** pentadactyl and semi-plantigrade pes imprint, longer than wide (FL = 33.4 cm;  
345 FW = 19.2 cm; FL/FW = 1.74). Digit III is the longest. It is slightly longer than II, whereas digit  
346 IV is shorter than II. Digit I is the shortest and is thinner than those of digit group II-IV. The total  
347 divarication I-IV is 22°; the angle between digit I and II is 8° and is equal to that between II and  
348 III but larger than II-IV (6°). Cross axis is nearly equal to 90°. Digit impressions are robust and  
349 pointed showing large sub-triangular claw marks. Two phalangeal pad impressions are present  
350 on each digit of group I-IV. The metatarsal-phalangeal portion is proximally arched and could be  
351 separated from digit V by a gap, or joined with it through a convex area, running from the  
352 basalmost portion of digit I to the medial digit V. Digit V shows a large oval impression joined  
353 to a rounded phalangeal-ungual portion, laterally spread out. In GT-7-2 and GT-7-3, pes digit V  
354 has a sub-triangular shape with a wider inner margin, almost aligned with the medial margin of  
355 digit I. Length of pes digits are: I) 118 mm; II) 173 mm; III) 186 mm; IV) 136 mm; V) 167 mm.

356 The manus is small, tetradactyl and digitigrade, wider than long (FL = 8.04 cm; FW = 13 cm;  
357 FL/FW = 0.62) and is placed in front of the pes. Digits are short and pointed. Digits II and III  
358 have nearly equal length and are longer than digits I and IV; the latter is moderately spread  
359 outward. Digit IV is possibly the shortest. Length of manus digits are: I) 49 mm; II) 74 mm; III)  
360 68 mm; IV) 43 mm.

361 The trackway, made by three consecutive manus-pes sets, shows a clear narrow gait (pace  
362 angulation 164°). Oblique pace is 59 cm, whereas double pace is 119 cm across. Manus-pes  
363 couples turned slightly outward with respect to the midline (from 10° to 15° on average).

364

365     **Discussion:** the ichnogenus *Isochirotherium* was erected by Haubold (1971a); its type  
366     ichnospecies *I. soergeli* (Haubold, 1967) comes, as for *Chirotherium barthii*, from the  
367     “Thüringischer Chirotheriensandstein” (Lower-Middle Triassic) of the Thuringia region  
368     (Germany). The ichnogenus is reported also from the Middle Triassic of Great Britain (Tresise &  
369     Sarjeant, 1997; King et al., 2005), from the Lower–Middle Triassic of North American  
370     Southwest (Peabody, 1948; Klein & Lucas, 2010), the Aiguilles Rouges Massif (Western Alps)  
371     on the border between Switzerland and France (Avanzini & Cavin, 2009; Klein et al., 2016) and  
372     from the Middle Triassic of North-East Italy (Avanzini & Leonardi, 2002).

373     The main diagnostic features of this ichnogenus, retained by our specimens are: i) the relative  
374     digit length, with digit II longer than IV and shorter than III; ii) a marked heteropody; iii) the pes  
375     pace angulation around 165°; iv) the weakly impressed distal portion of digit V and v) pes-  
376     manus couples outward rotation of about 15°. However, the studied trackway shows clear  
377     difference to most of the ichnospecies known to date. For example, the type ichnospecies *I.*  
378     *soergeli* Haubold, 1967 (Fig. 8o), has smaller absolute dimensions, thinner pes digit marks and,  
379     most importantly, display five clear digit impressions in the manus contrary to GT-7, where only  
380     tetradactyl manus were observed.

381     *Isochirotherium hessbergense* Haubold, 1971a (Fig. 8m) has also a pentadactyl manus and is  
382     clearly different from the material described in this paper for its digit group I-IV longer than  
383     wider and for the relative pes digit length, notably digit I is longer than IV.

384     *Isochirotherium demathieui* Haubold, 1971a (Fig. 8n) can be excluded for its pentadactyl  
385     manus and for the shorter distance between manus and pes.

386 *Isochirotherium coltoni* Peabody, 1948 (Fig. 8h) and *I. lomasi* Baird, 1954 (Fig. 8i) retain  
387 much slenderer digit impressions, especially in the pes imprint and most notably have manus  
388 tracks more internally placed than in the studied footprints. Interestingly *I. herculis* Egerton,  
389 1839 (Fig. 8e) has similar dimensions (i.e. FL longer than 30 cm) but can also be excluded for i)  
390 the tridactyl manus; ii) the digit group I-IV slightly wider than longer and iii) the manus imprint  
391 position, very close to that of the pes.

392 *Isochirotherium marshalli* Peabody, 1948 (Fig. 8f) shows similar features such as: i) the pes  
393 digit relative length; ii) the interdigital angles values; iii) the digit group I-IV as longer as wider;  
394 iv) the arched metatarsal-phalangeal portion; v) the configuration of digit V whose phalangeal  
395 portion is significantly smaller than the ovoidal and possibly tarsal-metatarsal pad. Nevertheless,  
396 the assignment to this ichnospecies is precluded by its pentadactyl manus.

397 *Isochirotherium inferni* Avanzini & Leonardi, 2002 from the Illyrian (late Anisian, Middle  
398 Triassic; Fig. 8g) of the Adige Valley (Bolzano, NE Italy) closely resembles the Gardetta  
399 specimens for: i) the arched metatarsal-phalangeal portion; ii) the position of the base of pes digit  
400 V, placed along the axis of digit III; iii) pes digit relative length; iv) cross axis equal to 90° v) pes  
401 angulation of about 160°; vi) positive rotation of manus-pes couples respect to the midline (10°-  
402 15°). However, pes digits are stouter and the manus is described as pentadactyl (even if in the  
403 outline drawing only four digits are clearly appreciable). The tracks referred to *Isochirotherium*  
404 *delicatum* Courel & Demathieu, 1976 and found in the Anisian-Ladinian deposits of Argentière  
405 (Ardèche, France; Courel & Demathieu, 1976; Courel et al., 1979; Demathieu, 1984; Gand,  
406 1978) and Gampempass (Southern Alps, Italy; Avanzini & Lockley, 2002) show less-thick digit  
407 impressions and a markedly reduced digits IV and V; the latter is also much more backward  
408 positioned if compared with the studied specimens.

409 We therefore erect the new ichnospecies *Isochirotherium gardettae* to describe a new and  
410 well-preserved *Isochirotherium* trackway that differs from all the other ichnospecies for all the  
411 features listed above.

412

## 413 TRACKMAKER IDENTIFICATION

414

415 Grounding on previous studies and new observations Bernardi et al. (2015) showed that  
416 chirotherian footprints, such as *Protochirotherium*, *Chirotherium*, *Brachychirotherium* and  
417 *Isochirotherium*, can be confidently attributed to archosauriforms, based on the presence of a  
418 digit IV shorter or as long as digit III. Being metatarsal length directly proportionate to digit  
419 length, this assumes that metatarsal IV is shorter than or as long as metatarsal III, a  
420 synapomorphy of the archosauriforms (Nesbitt, 2011). Other characters useful to identify  
421 archosauriforms traces are: i) the presence of a compact digit group I-IV; ii) a posterolateral  
422 positioned and strongly reduced digit V; iii) a massive metatarsal-phalangeal region, shorter than  
423 or as long as digit I. However, the first character occurs in archosauriforms and non  
424 archosauromorphs diapsids (Haubold, 1971a, 1971b; Smith & Evans, 1996) whereas the second  
425 is present in archosauriforms, lepidosaurs and basal archosauromorphs (Haubold, 1971a, 1971b;  
426 Evans & Wang, 2005; Gottman-Quesada & Sander, 2009). Other features suggesting an archosaur  
427 affinity for chirotherian footprints (observed also in the here described traces), are narrow  
428 trackways linked to the disposition of limbs under the body, and the presence of small manus  
429 relative to the pes, which indicate a possible early tendency toward bipedal posture and gate (see  
430 Haubold, 1971a, 1971b, 1984, 2006; Klein et al., 2010).

431 To reconstruct the hind- and fore-limb autopodial bones, we assumed an arthal position for  
432 the joint articulations within digital pad impressions (Fig. 9a).

433 In our opinion, the sub-elliptical to pyriform impression behind group I-IV in *Isochirotherium*  
434 could be the result of the coalescence of the impression of the phalangeal-metatarsal portion of  
435 digit V and of a thick fleshy pad beneath the astragalus, the calcaneus and some of the tarsal  
436 bones. Overall, the trackmaker's pes may have had a semi-plantigrade posture, as evidenced by  
437 the gap between digit group I-IV and digit V, corresponding to the part of the foot held up during  
438 locomotion. The manus has a marked digitigrade posture and its tetractyly might result by the  
439 fact that manual digit V likely held off the ground during the touch-down and weight bearing  
440 phases (*sensu* Manning, 2004).

441 The reconstructions thus obtained shows the following pes and manus phalangeal formulas:  
442 pes 2-3-4-4-1 and manus 1-2-3-3. They are compared with the anterior and posterior limbs of the  
443 main groups of archosauriforms known in the Triassic period (Huene, 1902; Broom, 1903; 1905;  
444 Romer, 1971; Welles, 1947; Young, 1964; Zhang, 1975; Peyer et al., 2008; Ezcurra et al., 2013;  
445 Sookias & Butler, 2013; Trotteyn et al., 2013).

446 The first considered non-archosaurian archosauriforms groups are Proterosuchidae (Ezcurra et  
447 al., 2013), Proterochampsidae (Trotteyn et al., 2013) and Euparkeriidae (Sookias & Butler,  
448 2013). In all the three representatives *Proterosuchus fergusi* Broom, 1903 (South Africa,  
449 Induan-?early Olenekian; Fig. 9e), *Chanaresuchus bonapartei* Romer, 1971 (Argentina,  
450 Ladinian; Fig. 9i) and *Euparkeria capensis* Broom, 1913 (South Africa, Anisian; Fig. 9h), the IV  
451 metatarsal has a length similar or greater than that of the III but the digit II is much shorter than  
452 digit III and nearly equal to digit IV, in contrast to what we observe in specimens GT-7-1, GT-7-

453 2 and GT-3. No fore- or hind limb bones are known for the Doswelliidae, another clade of non-  
454 archosaurian archosauriforms (Middle-Late Triassic; Sues et al., 2013).

455 Diedrich (2015) recently attributed the *Isochirotherium* tracks to *Arizonasaurus* Welles, 1947,  
456 a member of Poposauroidea (archosaurian archosauriforms) found in the Moenkopi Formation  
457 (Arizona, USA, Anisian,), from the same levels as *Isochirotherium* tracks. Unfortunately, no  
458 bones of the fore- and hind-limbs are known from *Arizonasaurus*, as well as from  
459 *Ctenosauriscus koeneni* (Huene, 1902) (Germany, latest Olenekian), the Lower Triassic  
460 poposauroid archosaur, and additionally findings are needed to test Diedrich's hypothesis.

461 The hind-limb bones are known in *Lotosaurus adentus* Zhang, 1975 (China, Ladinian; Fig.  
462 9d), another member of Poposauroidea with semi-plantigrade posture. If compared with the  
463 restored autopodium, it is characterized by larger fore-limbs, V digit positioned further forward,  
464 longer metatarsals of digit group I-IV and different digit proportions.

465 The pedal phalangeal relative length of the rauisuchid archosaur *Postosuchus alisonae* Peyer  
466 et al., 2008 (USA, Norian; Fig. 9c), is similar but all the five metatarsals are much longer,  
467 implying a digitigrade posture, as in the reconstruction proposed by Peyer et al. (2008).

468 *Postosuchus kirkpatricki* Chatterjee, 1985 (USA, Norian; Fig. 9b), is also characterized by  
469 very long metatarsals and thus excluded as a possible trackmaker. The smaller but complete  
470 skeleton of *Ticinosuchus ferox* Krebs, 1965 (see Lautenschlager & Desojo, 2011 for a review of  
471 the species) from the uppermost Anisian of Monte San Giorgio (southern Switzerland), shows  
472 long metatarsals and a digit IV longer than digit II and is commonly considered as the producer  
473 of *Chirotherium* trackway (Haubold, 1984, 1986).

474 By contrast, the hind limbs of the non-archosaurian archosauriform clade of Erythrosuchidae  
475 (Ezcurra et al., 2013) are characterized by relative digit length very similar to that outlined for

476 *Isochirotherium gardettae* and a pedal phalangeal formula that is approximately 2-3-4-5-3  
477 (Young, 1964; Cruickshank, 1978; Gower, 1996).

478 Metatarsals II and III are sub-equal and slightly longer than IV in *Erythrosuchus africanus*  
479 Broom, 1905 (South Africa, lower Anisian; Fig. 9f. See also Cruickshank, 1978; Gower, 1996).

480 Metatarsals II and III are the longest in *Shansisuchus shansisuchus* Young, 1964 (Fig. 9g),  
481 another member of Erythrosuchidae found in upper Anisian deposits of China; *S. shansisuchus*  
482 also possesses a hook-shaped proximal end of metatarsal V and its relative digit proportion  
483 closely fits that of our individual, but as for *E. africanus* digit V seems to be too forwardly  
484 positioned. However, digit V impression in *I. gardettae* likely records only the distal metatarsal  
485 and phalangeal (ungual) portions. During locomotion the former was held off the ground  
486 whereas the latter was likely being retracted due to the presence of a thick fleshy pad beneath  
487 calcaneum and astragalus.

488 The morphology of the acetabulum and proximal end of the femur in erythrosuchids suggests  
489 a distinctly sprawling gait (Gower, 2003; Ezcurra et al., 2013), that clashes with the narrow  
490 trackway seen in *I. gardettae*. Nevertheless, the prominence of metatarsal II and III is evidenced  
491 only in non-archosaurian archosauriforms (Gower, 1996) and thus an individual belonging to this  
492 group, possibly a yet unknown taxon and with a more erect stance and characterized by a marked  
493 heteropody, is the most suitable producer (Fig. 10).

494

## 495 **BIOCHRONOLOGY AND BIOGEOGRAPHY**

496 The Gardetta ichnoassemblage represented by *Chirotherium* and *Isochirotherium* is typical  
497 for terrestrial deposits of the late Olenekian and early Anisian (Klein & Haubold, 2007) and the  
498 Gardetta chirotheriid tracks correlate with the international *Chirotherium barthii* Assemblage

499 Zone of Klein & Lucas (2010a). This biochron is characterized by the occurrence of  
500 *Chirotherium* and *Isochirotherium*, but also by two other ichnogenera not present at Gardetta,  
501 *Rotodactylus*, and *Synaptychium*. The *Chirotherium barthii* Assemblage Zone ranges from the  
502 late Early to early Middle Triassic (late Olenekian – early Anisian), and independently confirms  
503 the Early Triassic (?Olenekian) age, derived by stratigraphic correlation with other sections in  
504 the Briançonnais of the Western Alps.

505 The Gardetta outcrop enlarges also the knowledge on biogeography of archosaurs in the  
506 Lower Triassic of Europe, so far based on archosaur ichnosites discovered in Italy (Val Marenca,  
507 Santi et al., 2015; Sardinia, Citton et al., 2020), Spain (Moncayo and Tagamanent, Díaz-Martínez  
508 & Pérez-García, 2012), Switzerland (Cascade d'Emaney and Vieux Emosson; Cavin et al.,  
509 2012), Austria (Drau Range; Krainer et al., 2012), Germany (Bundsandstein; Klein & Haubold,  
510 2007) and Poland (Wióry, Holy Cross Mountains, Klein & Niedźwiedzki, 2012).

511 Early Triassic erythrosuchid skeletal fossils are known from the late Olenekian of Russia,  
512 South Africa, China and India (see Gower, 2003; Ezcurra et al., 2013, 2019, 2020; Gower et al.,  
513 2014; Ezcurra, 2016). The Gardetta ichnosite testifies the presence of erythrosuchids and more  
514 generally of Archosauriformes at low latitudes (11.8° N) also during the Early Triassic (Fig. 11).  
515 This supports the conclusions of Bernardi et al. (2015, 2018) that Early Triassic ichnosites are  
516 mainly distributed along the tropics, contrasting the pattern described by skeletal findings and the  
517 hypothesis of a low-latitude vacancy of continental tetrapods during or soon after the PTME  
518 (Sun et al., 2012).

519

## 520 **Discussion and conclusions**

521 The Gardetta ichnosite is characterized by archosaur footprints assigned to *Chirotherium* isp.  
522 and to the new ichnospecies *Isochirotherium gardettae* ichnosp. nov. They represent the first  
523 record of terrestrial tetrapods in the Briançonnais domain of the Western Alps and expand the  
524 record of archosaur footprints in the Lower Triassic of Central Europe.

525 The morphological characters of the tracks assigned to *Isochirotherium gardettae* ichnosp.  
526 nov. suggest a non-archosaurian archosauriform (Erythrosuchidae?) as possible trackmaker  
527 candidate (even though the presence of crown-archosaurs cannot be excluded), thus providing  
528 crucial information about continental tetrapod occurrence in Europe in the Early Triassic. Based  
529 on a phylogenetic dataset made by 108 middle Permian–early Late Triassic species, Ezcurra &  
530 Butler (2015) investigate principal patterns of early archosauromorph biodiversity change across  
531 the Permo-Triassic mass extinction. The study, performed using phylogenetic diversity,  
532 morphological disparity, number of species and rates of phenotypic evolution across 35 million  
533 years of early archosauromorph evolution, indicates consistent phylogenetic diversification of  
534 the clade in the Olenekian. In particular, the basal diversification of main taxa, which include  
535 erythrosuchids, rhynchosauroids and tanystropheids, resulted in significantly high evolutionary  
536 rates, with a diversification interpreted by the authors as a radiative response to vacant ecological  
537 space, made available by the EPME (Ezcurra & Butler, 2015). If the trackmakers' attribution for  
538 the here described footprints is correct, the material from Gardetta could represent an evidence  
539 from Europe of such radiation, with an archosauromorph fauna composed at least by  
540 ?erythrosuchids (*Isochirotherium gardettae*) and pseudosuchids (*Chirotherium* isp.). Such clades  
541 as putative trackmaker for the Gardetta traces are well compatible with an Early Triassic (likely  
542 late Early Triassic) age, considering that the early history of Archosauriformes is represented  
543 essentially by members of Proterosuchidae and Erythrosuchidae (Charig & Reig, 1970;

544 Cruickshank, 1972; Charig & Sues, 1976; Gower & Sennikov, 2000; Gower, 2003; Ezcurra et  
545 al., 2013).

546 Following the huge Permo-Triassic biotic crisis, unfavorable environmental conditions  
547 characterized much of the Early Triassic, testifying one of the slowest recoveries for ecosystems  
548 after an extinction in Earth history. A period between five and nine million years for a full  
549 recovery has been proposed in several contributions (Hallam, 1991; Erwin, 1992, 2001; Payne et  
550 al., 2004, 2011; Algeo et al., 2011; Whiteside & Ward, 2011), inferring a fully restored complex  
551 ecosystems only at the beginning of the Middle Triassic (see Chen & Benton, 2012). Such long  
552 recovery time led to a revolution on both marine and terrestrial ecosystems (Chen & Benton,  
553 2012), with a major influence in the evolution of crucial vertebrates clades in the rest of  
554 Mesozoic and Cenozoic eras (Sepkoski, 1984; Benton, 2010). The recovery period led to the  
555 emergence of totally new groups, with a rapid diversification of several lineages of sauropsid  
556 both on sea and land (Nesbitt et al., 2010; Butler et al., 2011; Gower et al., 2014; Scheyer et al.,  
557 2014; Motani et al., 2015a, 2015b; Peecook et al., 2018). Avemetatarsalians (which include  
558 dinosaurs and pterosaurs) originated in this period (Brusatte et al., 2010; Nesbitt et al., 2010;  
559 Chen & Benton, 2012; Benton et al., 2014), along with the evolution of crucial modern group  
560 ancestors, including crocodiles, lizards, turtles, frogs and mammals. All these aspects highlight  
561 the crucial importance of the Early Triassic in the ecosystems restructuring after the Permo-  
562 Triassic mass extinction.

563 Retallack et al. (2011) propose that the long recovery from the mass extinction was strongly  
564 influenced by repeated greenhouse crises during the Early Triassic, with consistent negative  
565 excursions in carbon isotope ratios indicating at least five greenhouse crises in the 5 Myr  
566 following the EPME (Induan-Anisian) (see Kidder & Worsley, 2004; Retallack, 2005, 2009,

567 2013; Gaisby et al., 2011; Retallack et al., 2011; Sun et al., 2012; Chen & Benton, 2012). In this  
568 regard, according to Sun et al. (2012) the entire Early Triassic was characterized by temperatures  
569 consistently in excess ~~with respect to~~ the modern equatorial annual sea surface temperatures  
570 (SSTs), thus exceeding a tolerable threshold for life in both oceans and ~~land~~. Inferring SSTs  
571 approaching 40°C, according to Sun et al. (2012) the temperature on land very likely fluctuated  
572 to even higher levels, with terrestrial tetrapods generally absent between 30°N and 40°S in the  
573 Early Triassic.

574 In this framework, and although some uncertainties on the chronological attribution persists,  
575 the Gardetta ichnosite provides important evidence to the low latitude distribution of archosaurus  
576 during the Early Triassic period, soon after the PTME, confirming the pattern described by  
577 Bernardi et al. (2018). In particular, the new discovery provides further evidence for an early  
578 recovery terrestrial ecosystems and the presence at low latitudes of archosauriformes during the  
579 Early Triassic. Such evidences support a model in which the EPME did not completely vacate  
580 low-latitude lands from tetrapods that, therefore would, have been able to cope with the extreme  
581 hot temperatures of Pangaea mainland.

582 According to Botha and Smith (2006), Archosauromorpha (along with Procolophonomorpha)  
583 could be pre-adapted to extremely arid and hot environment conditions, considering that extant  
584 reptiles rarely drink water, excrete quite dry fecal pellets, and are characterized by solute-linked  
585 water reabsorption mechanisms, water-resistant integument and low ventilation rates (Withers,  
586 1992; Pough et al., 1996). Such physiological aspects and water conserving mechanisms,  
587 probably suggest that the archosaurus response to the extreme hot condition of the Early Triassic  
588 (Benton, 2018) have probably been much more efficient and ~~plastic~~ than previously thought, and

589 did not necessarily imply massive dispersal towards higher latitudes as previously suggested  
590 (Sun et al., 2012).

591 Different anatomical features described above indicate ~~a possible~~ ?Erythrosuchids as the most  
592 probable ~~trackmaker~~ for the new described ichnospecies *Isochirotherium gardettae*. This  
593 attribution can also be supported by track parameters such a narrow trackway and high pace  
594 angulation, which indicate a more upright posture with respect to a classic plesiomorphic  
595 sprawling gait (see Kubo & Benton, 2007). In particular, according to Ezcurra et al. (2013),  
596 erythrosuchids were heavily built and characterized by a probably less sprawling gait, when  
597 compared to the condition observed in proterosuchids. The narrow trackway, along with  
598 consistently high pace angulation in the Gardetta material, also confirm the statement by Kubo &  
599 Benton (2009) that, even if proterosuchids and erythrosuchids are traditionally considered as  
600 sprawlers, ichnological evidences indicate that more derived erect-limbed ~~archosaurian~~ already  
601 evolved in the Early Triassic; the latter conclusion is also supported ~~on the base of~~ ghost ranges  
602 from cladograms (Sereno, 1991; Benton, 1999), and fragmentary materials from Russia (Gower  
603 & Sennikov, 2000).

604 To date, Erythrosuchids are totally unknown from North America and Europe, being  
605 described only from Russia, South Africa, China and India (see Gower, 2003; Ezcurra et al.,  
606 2013, 2019, 2020; Gower et al., 2014; Ezcurra, 2016). ~~The~~ material from the Lower Triassic  
607 deposits of Gardetta ~~thus~~ could represent the first occurrence of the clade in Europe, although, as  
608 already pointed out, the attribution is for the moment only tentative, and new studies are  
609 underway to better constrain the identity of the zoological trackmaker.

610 The planned future excavations in the Gardetta ichnosite will hopefully provide additional  
611 data to improve our knowledge of the evolutionary history of Archosauriformes in the aftermath  
612 of the EPME.

613

614 **ELECTRONIC SUPPLEMENTARY MATERIAL**

615 This article contains electronic supplementary material.

616

617 **ACKNOWLEDGMENTS**

618 We warmly thank the Associazione Escarton that generously supported by this research during  
619 the field campaigns held in 2009, 2017 and 2018. A special thanks to Giovanni Raggi for his  
620 valuable and constant support during the field works and the project organisation. We  
621 acknowledge insightful discussions with A. d'Atri (University of Torino). The authors wish also  
622 to thank Dr. Debora Rocchietti (Soprintendenza Archeologia Belle Arti e Paesaggio per le  
623 province di Alessandria, Asti e Cuneo) and Dr. Attilio Dalmasso (Museo dei fossili in San Rocco  
624 di Bernezzo) and Fabio Manucci for video production and artwork. Finally, a special thank is  
625 also due to Hanna Luginbühl for her help in mapping 2009 and to Cecilia Gomiero, Jacopo  
626 Valori and Nicolò Amoruso for their precious help during 2018 fieldwork.

627 This paper is part of the project 'The end-Permian mass extinction in the Southern and Eastern  
628 Alps: extinction rates versus taphonomic biases in different depositional environments' financed  
629 by the Euregio Science Fund (call 2014, IPN16) of the Europaregion Euregio.

630

631 **REFERENCES**

632 **Algeo TJ, Chen ZQ, Fraiser ML, Twitchett RJ. 2011.** Terrestrial–marine teleconnections in  
633 the collapse and rebuilding of Early Triassic marine ecosystems. *Palaeogeography,*  
634 *Palaeoclimatology, Palaeoecology* **308(1-2)**:1-11.

635 **Alroy J. 2003.** Global databases will yield reliable measures of global biodiversity. *Paleobiology*  
636 **29(1)**:26-29.

637 **Avanzini M, Cavin L. 2009.** A new *Isochirotherium* trackway from the Triassic of Vieux  
638 Emosson, SW Switzerland: stratigraphic implications. *Swiss Journal of Geosciences* **102**:353-  
639 361.

640 **Avanzini M, Leonardi G. 2002.** *Isochirotherium inferni* ichnosp. n. in the upper Anisian  
641 (Illyrian) of Adige Valley (bozen, Italy). *Bollettino della Società Paleontologica Italiana*  
642 **41**:41-50.

643 **Avanzini M, Lockley M. 2002.** Middle Triassic archosaur population structure: interpretation  
644 based on *Isochirotherium delicatum* fossil footprints (Southern Alps, Italy).  
645 *Palaeogeography, Palaeoclimatology, Palaeoecology*, **185(3-4)**: 391-402.

646 **Avanzini M, Mietto P. 2008.** Lower and Middle Triassic footprint-based biochronology in the  
647 Italian Southern Alps. *Oryctos* **8**:3-13.

648 **Baird D. 1954.** *Chirotherium lulli*, a pseudosuchian reptile from New Jersey. *Museum of*  
649 *Comparative Zoology Bulletin* **111**:165-192.

650 **Baud A. 1976.** Les terriers de Crustacés décapodes et l'origine de certains facies du Trias  
651 carbonaté. *Eclogae Geologicae Helvetiae* **69(2)**:415-424.

652 **Baud A, Plasencia P, Hirsch F, Richoz S. 2016.** Revised middle Triassic stratigraphy of the  
653 Swiss Prealps based on conodonts and correlation to the Briançonnais (Western Alps). *Swiss*  
654 *Journal of Geosciences* **109**:365–377.

655 **Benton MJ. 1999.** *Scleromochlus taylori* and the origin of dinosaurs and pterosaurs.

656     *Philosophical Transactions of the Royal Society of London. Series B: Biological Sciences*

657     **354(1388):**1423-1446.

658 **Benton MJ. 2003.** When life nearly died: the greatest mass extinction of all time. Thames &

659     Hudson, London.

660 **Benton MJ. 2010.** The origins of modern biodiversity on land. *Philosophical Transactions of the*

661     *Royal Society B: Biological Sciences* **365(1558):**3667-3679.

662 **Benton MJ. 2018.** Hyperthermal-driven mass extinctions: killing models during the Permian–

663     Triassic mass extinction. *Philosophical Transactions of the Royal Society A* **376:**20170076.

664 **Benton M, Newell AJ. 2014.** Impacts of global warming on Permo-Triassic terrestrial

665     ecosystems. *Gondwana Research* **25:**1308–1337.

666 **Benton MJ, Twitchett RJ. 2003.** How to kill (almost) all life: the end-Permian extinction event.

667     *Trends in Ecology & Evolution* **18:**358–365.

668 **Benton MJ, Forth J, Langer MC. 2014.** Models for the rise of the dinosaurs. *Current Biology*

669     **24:**R87–R95.

670 **Bernardi M, Petti FM, Benton MJ. 2018.** Tetrapod distribution and temperature rise during the

671     Permian- Triassic mass extinction. *Proceedings of the Royal Society of London B*

672     **285:**20172331.

673 **Bernardi M, Klein H, Petti FM, Ezcurra MD. 2015.** The Origin and Early Radiation of

674     Archosauriforms: Integrating the Skeletal and Footprint Record. *PLoS ONE* **10(6):**e0128449.

675 **Berner RA. 2002.** Examination of hypotheses for the Permo-Triassic boundary extinction by

676     carbon cycle modeling. *Proceedings of the National Academy of Sciences, U.S.A.* **99:**4172–

677     4177.

678 **Bertok C, Martire L, Perotti E, d'Atri A, Piana F. 2012.** Kilometre-scale palaeoescarpments  
679 as evidence for Cretaceous synsedimentary tectonics in the External Briançonnais Domain  
680 (Ligurian Alps, Italy). *Sedimentary Geology* **251**:58-75.

681 **Botha J, Smith RMH. 2006.** Rapid vertebrate recuperation in the Karoo Basin of South Africa  
682 following the end-Permian extinction. *Journal of African Earth Sciences* **45**:502–514.

683 **Broom R. 1903.** On a new reptile (*Proterosuchus fergusi*) from the Karoo beds of Tarkastad,  
684 South Africa. *Annals of the South African Museum* **4**:159-164.

685 **Broom R. 1905.** Notice of some new reptiles from the Karoo Beds of South Africa. *Records of*  
686 *the Albany Museum* **1**:331-337.

687 **Broom R. 1913.** Note on *Mesosuchus browni*, Watson, and on a new South African Triassic  
688 pseudosuchian (*Euparkeria capensis*). *Records of the Albany Museum* **2**: 394-396.

689 **Brusatte SL, Benton MJ, Desojo JB, Langer MC. 2010.** The higher-level phylogeny of  
690 Archosauria (Tetrapoda: Diapsida). *Journal of Systematic Palaeontology* **8**(1):3-47.

691 **Butler RJ, Brusatte SL, Reich M, Nesbitt SJ, Schoch RR, Hornung JJ. 2011.** The sail-  
692 backed reptile *Ctenosauriscus* from the latest Early Triassic of Germany and the timing and  
693 biogeography of the early archosaur radiation. *PLoS ONE* **6**(10):e25693.

694 **Caby R, Galli J. 1964.** Existence de cinérites et tufs volcaniques dans le Trias moyen de la zone  
695 briançonnaise. *Comptes Rendus de l'Académie des Sciences de Paris* **259**:417-420.

696 **Carrano MT, Wilson JA. 2001.** Taxon distributions and the tetrapod track record. *Paleobiology*  
697 **27**(3):564-582.

698 **Carraro F, Dal Piaz GV, Franceschetti B, Malaroda R, Sturani C, Zanella E. 1970.** Carta  
699 Geologica del massiccio dell'Argentera alla scala 1: 50.000 e Note Illustrative. *Memorie della*  
700 *Società Geologica Italiana* **9**:557-663.

701 **Cassinis G, Perotti C, Santi G.** 2018. Post-Variscan Verrucano-like deposits in Italy, and the  
702 onset of the alpine tectono-sedimentary cycle. *Earth-Science Reviews* **185**:476-497.

703 **Cavin L, Avanzini M, Bernardi M, Piuz A, Proz PA, Meister C, Boissonnas J, Meyer CA.**  
704 2012. New vertebrate trackways from the autochthonous cover of the Aiguilles Rouges  
705 Massif and reevaluation of the dinosaur record in the Valais, SW Switzerland. *Swiss Journal*  
706 *of Palaeontology* **131**:317-324.

707 **Charig AJ, Reig OA.** 1970. The classification of the Proterosuchia. *Biological Journal of the*  
708 *Linnean Society* **2(2)**:125-171.

709 **Charig AJ, Sues H-D.** 1976. Proterosuchia. In: Kuhn, O. (ed.) *Handbuch der Paläoherpetologie*  
710 13. Gustav Fischer, Stuttgart, 11–39.

711 **Chatterjee S.** 1985. *Postosuchus*, a new thecodontian reptile from the Triassic of Texas and the  
712 origin of tyrannosaurs. *Philosophical Transactions of the Royal Society of London B* **309**:395-  
713 460.

714 **Chen ZQ, Benton MJ.** 2012. The timing and pattern of biotic recovery following the end-  
715 Permian mass extinction. *Nature Geoscience* **5(6)**:375-383.

716 **Citton P, Ronchi A, Nicosia U, Sacchi E, Maganuco S, Cipriani A, Innamorati G, Zuccari**  
717 **C, Manucci F, Romano M.** 2020. Tetrapod tracks from the Middle Triassic of NW Sardinia  
718 (Nurra region, Italy). *Italian Journal of Geosciences* **139(2)**:309-320.

719 **Costamagna LG.** 2013. Middle Triassic carbonate lithostratigraphy of the Southern  
720 Briançonnais (Cottian Alps, Italy) and comparison with the surrounding areas. *GeoActa* **12**:1-  
721 24.

722 **Costamagna LG, Barca S, Nervo R.** 2002. Analisi di facies della successione carbonatica  
723 mediotriassica del Dominio Brianzinese fra le valli Stura e Maira (Alpi Occidentali, Cuneo,

724 Italia): La sezione del Vallone del Preit. In: Fioraso G., Malusà M., Mosca P. & Tallone S.  
725 (eds.) - 81<sup>a</sup> Riunione estiva SGI, Riassunti delle Comunicazioni orali e dei poster: 110-111,  
726 Torino.

727 **Courel L, Demathieu G. 1976.** Une ichnofaune reptilienne remarquable dans les grès Triasique  
728 de Largentière (Ardèche, France). *Palaeontogr. A* **151**: 194–216.

729 **Courel L, Demathieu G, Gall JC. 1979.** Figures sédimentaires et traces d'origine biologique du  
730 Trias moyen de la bordure orientale du Massif Central. Signification sédimentologique et  
731 paleoécologique. *Geobios* **12**: 379-397.

732 **Cruickshank ARI. 1972.** The proterosuchian thecodonts. In: Joysey, K. A. & Kemp, T. S. (eds)  
733 Studies in Vertebrate Evolution. Oliver and Boyd, Edinburgh, 89–119.

734 **Cruickshank ARI. 1978.** The pes of *Eythrosuchus africanus* Broom. *Zoological Journal of the*  
735 *Linnean Society* **62**:161-177.

736 **d'Atri A, Piana F, Barale L, Bertok C, Martire L. 2016.** Geological setting of the southern  
737 termination of Western Alps. *International Journal of Earth Sciences* **105**(6):1831-1858.

738 **Decarlis A, Lualdi A. 2009.** A sequence stratigraphic approach to a Middle Triassic shelf-slope  
739 complex of the Ligurian Alps (Ligurian Briançonnais, Monte Carmo-Rialto unit, Italy).  
740 *Facies* **55**:267-290.

741 **Decarlis A, Dallagiovanna G, Lualdi A, Maino M, Seno S. 2013.** Stratigraphic evolution in the  
742 Ligurian Alps between Variscan heritages and the Alpine Tethys opening: A review. *Earth-*  
743 *Science Reviews* 125:43-68.

744 **Decarlis A, Manatschal G, Haupert I, Masini E 2015.** The tectono-stratigraphic evolution of  
745 distal, hyper-extended magma-poor conjugate rifted margins: Examples from the Alpine  
746 Tethys and Newfoundland–Iberia. *Marine and Petroleum Geology* **68**:54-72.

747 **Demathieu G. 1970.** Les empreintes de pas de vertébrés du Trias de la bordure Nord-Est du  
748 Massif Central. Cahiers de Paléontologie CRNS Paris, 211 p.

749 **Demathieu G. 1984.** Une ichnofaune du Trias moyen du basin de Lodève (Hérault, France).  
750 *Ann. Paleontol. (Vertebr.-Invertebr.)* **70:** 247-273.

751 **Demathieu G, Weidmann M. 1982.** Les empreintes de pas de reptiles dans le Trias du Vieux  
752 Emosson (Finhaut, Valais, Suisse). *Eclogae Geologicae Helvetiae* **75:**721-757.

753 **Díaz-Martínez I, Pérez-García A. 2012.** Historical and comparative study of the first Spanish  
754 vertebrate paleoichnological record and bibliographic review of the Spanish chirotheriid  
755 footprints. *Ichnos*, **19(3):** 141-149.

756 **Díaz-Martínez I, Castanera D, Gasca JM, Canudo JI. 2015.** A reappraisal of the Middle  
757 Triassic chirotheriid *Chirotherium ibericus* Navas, 1906 (Iberian Range, NE Spain), with  
758 comments on the Triassic tetrapod track biochronology of the Iberian Peninsula. *PeerJ*  
759 **3:**1044.

760 **Diedrich C. 2015.** *Isochirotherium* trackways, their possible trackmakers (*?Arizonasaurus*):  
761 intercontinental giant archosaur migrations in the Middle Triassic tsunami-influenced  
762 carbonate intertidal mud flats of the European Germanic Basin. *Carbonates and Evaporites*  
763 **30:**229-252.

764 **Egerton PG. 1839.** On two casts in sandstone of impression of the Hind Foot of a gigantic  
765 *Cheirotherium*, from the New red sandstone of Cheshire. *The London and Edinburgh*  
766 *Philosophical Magazine and Journal of Science, 3rd series* **14(75):**151-158.

767 **Erwin DH. 1992.** A preliminary classification of evolutionary radiations. *Historical Biology*  
768 **6:**133-147.

769 **Erwin DH. 1993.** The Great Paleozoic Crisis, Life and Death in the Permian. Colombia  
770 University Press, New York, 327 pp.

771 **Erwin DH. 2001.** Lessons from the past: biotic recoveries from mass extinctions. *Proceedings of*  
772 *the National Academy of Sciences* **98(10)**:5399-5403.

773 **Evans SE, Wang Y. 2005.** *Dalinghosaurus*, a lizard from the Early Cretaceous Jehol Biota of  
774 north- east China. *Acta Paleontologica Polonica* **50**:725-742.

775 **Ezcurra MD. 2016.** The phylogenetic relationships of basal archosauromorphs, with an  
776 emphasis on the systematics of proterosuchian archosauriforms. *PeerJ* **4**:e1778.

777 **Ezcurra MD, Butler RJ. 2015.** Taxonomy of the proterosuchid archosauriforms (Diapsida:  
778 Archosauromorpha) from the earliest Triassic of South Africa, and implications for the early  
779 archosauriform radiation. *Palaeontology* **58(1)**:141-170.

780 **Ezcurra MD, Butler RJ, Gower DJ. 2013.** 'Proterosuchia': the origin and early history of  
781 Archosauriformes. *Geological Society, London, Special Publications* **379(1)**:9-33.

782 **Ezcurra MD, Gower DJ, Sennikov AG, Butler RJ. 2019.** The osteology of the holotype of the  
783 early erythrosuchid *Garjainia prima* Ochev, 1958 (Diapsida: Archosauromorpha) from the  
784 upper Lower Triassic of European Russia. *Zoological Journal of the Linnean Society*  
785 **185**:717–783.

786 **Ezcurra MD, Jones AS, Gentil AR, Butler RJ. 2020.** Early Archosauromorphs: The Crocodile  
787 and Dinosaur Precursors. *Encyclopedia of Geology*, 2nd edition.

788 **Ezcurra MD, Velozo P, Meneghel M, Piñeiro G. 2015.** Early archosauromorph remains from  
789 the Permo-Triassic Buena Vista Formation of north-eastern Uruguay. *PeerJ* **3**:e776.

790 **Feldmann M, Furrer H, Glarus K. 2009.** Die Saurierspuren am Tödi und ihre geologische  
791 Umgebung. *Mitteilungen der Naturforschenden Gesellschaft des Kantons Glarus* **18**:28-37.

792 **Fortuny J, Bolet A, Selles AG, Cartanya J, Galobart A. 2011.** New insights on the Permian  
793 and Triassic vertebrates from the Iberian peninsula with emphasis on the Pyrenean and  
794 Catalonian basins. *Journal of Iberian Geology* **37**(1):65-86.

795 **Gand G. 1978.** Interprétations paléontologique et paléoécologique d'un sixième assamblage à  
796 traces de reptiles des carrières triasiques de St.-Sernin-du Bois (Autunois, France).  
797 Conclusions générales à étude du gisement. *Bulletin de la Société d'Historie Naturelle*  
798 *d'Autun* **87**: 9–29.

799 **Gand G. 1979.** Description de deux nouvelles traces d'*Isochirotherium* observées dans les grès  
800 du Trias moyen de Bourgogne. *Bull. Soc. Hist. Nat. Creusot* **37**: 13–25.

801 **Gidon M. 1958a.** Nouvelles observations sur la zone briançonnaise au delà de la frontière  
802 franco-italienne (Bassin de la Haute Maira, Province de Cuneo). *Trav. Lab. Géol. Univ.*  
803 *Grenoble* **34**:153-167.

804 **Gidon M. 1958b.** La Zone Briançonnaise en Haute Ubaye (Basses-Alpes) et son prolongement  
805 au Sud-Est. PhD Thesis. Faculté des Sciences de l'Université de Grenoble, 272 pp.

806 **Gidon M. 1972.** Les chainons briançonnais et subbriançonnais de la rive gauche de la Stura  
807 entre la Val de l'Arma (province de Cuneo-Italie). *Géologie Alpine* **48**(1):87-120.

808 **Gidon M. 1978.** Carte géologique détaillée de la France à l'échelle 1/50.000, feuille Larche, 1°  
809 édition. Bureau de Recherche Géologique et Minière, Orléans, with explanatory notes, pp. 1–  
810 28.

811 **Golden Software 2002.** Surfer version 8.0: surface mapping system.

812 **Gottmann-Quesada A, Sander PM. 2009.** A redescription of the early archosauromorph  
813 *Protorosaurus speneri* Meyer, 1832 and its phylogenetic relationships. *Palaeontographica*  
814 *Abteilung A* **287**:123-220.

815 **Gower DJ. 1996.** The tarsus of erythrosuchid archosaurs, and implications for early diapsid  
816 phylogeny. *Zoological Journal of the Linnean Society* **116**(4):347-375.

817 **Gower DJ. 2003.** Osteology of the early archosaurian reptile *Erythrosuchus africanus* Broom.  
818 *Annals of the South African Museum* **110**:1-88.

819 **Gower DJ, Sennikov AG. 2000.** Early Archosaurs from Russia. In: Benton MJ, Shishkin MA,  
820 Unwin DM, Kurochkin EN, editors. *The Age of Dinosaurs in Russia and Mongolia*.  
821 Cambridge University Press, Cambridge. pp. 140–159.

822 **Gower DJ, Hancox PJ, Botha-Brink J, Sennikov AG, Butler RJ. 2014.** A new species of  
823 *Garjainia* Ochev, 1958 (Diapsida: Archosauriformes: Erythrosuchidae) from the Early  
824 Triassic of South Africa. *PLoS One* **9**(11):e111154.

825 **Grasby SE, Sanei H, Beauchamp B. 2011.** Catastrophic dispersion of coal fly ash into oceans  
826 during the latest Permian extinction. *Nature Geoscience* **4**(2):104.

827 **Hallam A. 1991.** Why was there a delayed radiation after the end-Palaeozoic extinctions?.  
828 *Historical Biology* **5**(2-4):257-262.

829 **Haubold H, Klein H. 2002.** Chirotherien und Grallatoriden aus der Unteren bis Oberen Trias  
830 Mitteleuropas und die Entstehung der Dinosauria. *Hallesches Jahrbuch für  
831 Geowissenschaften B* **24**:1-22.

832 **Haubold H. 1967.** Eine Pseudosuchier- Fährtenfauna aus dem buntsandstein südthüringens.  
833 *Hallesches Jahrbuch für Mitteldeutsche Erdgeschichte* **8**:12-48.

834 **Haubold H. 1984.** Saurierfährten. A. Ziemsen Verlag, Wittenberg, 232 pp.

835 **Haubold H. 1971a.** Die Tetrapodenfährten des Buntsandsteins. *Paläontologische Abhandlungen  
836 A* **4**(3):395-548.

837 **Haubold H. 1971b.** *Ichnia Amphibiorum et Reptiliorum fossilium*. Encyclopedia of  
838 Paleoherpetology **18**:1-124.

839 **Haubold H. 1970.** Die Tetrapodenfährten des Germanischen Buntsandsteins und ihre  
840 Äquivalente in der gesamten Trias. *Paläontologische Abhandlungen, Abteilung A,*  
841 *Palaeozoologie*, 4.

842 **Haubold H. 1984.** Saurierfährten. Wittenberg, Ziemsen, 231 p.

843 **Haubold H. 1986.** Archosaur footprints at the terrestrial Triassic–Jurassic transition. 190–201.

844 In Padian K. (ed.). *The beginning of the Age of Dinosaurs: Faunal change across the Triassic–*  
845 *Jurassic boundary*. Cambridge University Press, Cambridge, 378 pp.

846 **Haubold H. 2006.** Die Saurierfährten *Chirotherium barthii* Kaup, 1835—das Typusmaterial aus  
847 dem Buntsandstein bei Hildburghausen/Thüringen und das Chirotherium-Monument.

848 *Veröffentlichungen Naturhistorisches Museum Schleusingen* **21**:3–31.

849 **Huene F. von 1902.** Übersicht über die Reptilien der Trias. *Geologische und Paläontologische*  
850 *Abhandlungen* **10**:1-84.

851 **Joachimski MM, Lai X, Shen S, Jiang H, Luo G, Chen B, Chen J, Sun Y. 2012.** Climate  
852 warming in the latest Permian and the Permian–Triassic mass extinction. *Geology* **40**:195–  
853 198.

854 **Kaup JJ. 1835.** Über Tierfährten bei Hildburghausen. *Neues Jahrbuch für Mineralogie,*  
855 *Geologie und Paläontologie* 1835, 327–328.

856 **Kidder DL, Worsley TR. 2004.** Causes and consequences of extreme Permo–Triassic warming  
857 to globally equitable climate and relation to the Permo–Triassic extinction and recovery.

858 *Palaeogeography, Palaeoclimatology, Palaeoecology* **203**(3–4):207–237.

859 **King MJ, Sarjeant WAS, Thompson DB, Tresise G. 2005.** A revised systematic  
860 ichnotaxonomy and review of the vertebrate footprint ichnofamily Chirotheriidae from the  
861 British Triassic. *Ichnos* **12**:241-299.

862 **Klein H, Lucas SG. 2010a.** Tetrapod footprints and their use in biostratigraphy and  
863 biochronology of the Triassic. In Lucas, S.G. (ed.), The Triassic timescale. *Geological Society*  
864 *of London Special Publications* **334**:419-446.

865 **Klein H, Niedźwiedzki G. 2012.** Revision of the Lower Triassic tetrapod ichnofauna from  
866 Wióry, Holy Cross Mountains, Poland. *New Mexico Museum of Natural History and Science,*  
867 *Bulletin* **56**:1-62.

868 **Klein H, Haubold H. 2007.** Archosaur footprints-potential for biochronology of Triassic  
869 continental sequences. *New Mexico Museum of Natural History and Science Bulletin* **41**:120-  
870 130.

871 **Klein H, Lucas SG. 2010.** Review of the tetrapod ichnofauna of the Moenkopi Formation/Group  
872 (Early-Middle Triassic) of the American Southwest. *New Mexico Museum of Natural History*  
873 *and Science Bulletin* **50**:1-67.

874 **Klein H, Voigt S, Hminna A, Saber H, Schneider J, Hmich D. 2010.** Early Triassic archosaur-  
875 dominated footprint assemblage from the Argana Basin (western High Atlas, Morocco).  
876 *Ichnos* **17(3)**:215-227.

877 **Klein H, Voigt S, Saber H, Schneider JW, Hminna A, Fischer J, Lagnaoui A, Brosig A.**  
878 **2011.** First occurrence of a Middle Triassic tetrapod ichnofauna from the Argana Basin  
879 (Western High Atlas, Morocco). *Palaeogeography, Palaeoclimatology, Palaeoecology*  
880 **307**:218-231.

881 **Klein H, Wizevich MC, Thüring B, Marty D, Thüring S, Falkingham P, Meyer CA. 2016.**

882 Triassic chirotheriid footprints from the Swiss Alps: ichnotaxonomy and depositional  
883 environment (Cantons Wallis & Glarus). *Swiss Journal of Palaeontology*, **135**(2): 295-314.

884 **Knoll AH, Bambach RK, Payne JL, Pruss S, Fischer WW. 2007.** Paleophysiology and end-  
885 Permian mass extinction. *Earth and Planetary Science Letters* **256**(3-4):295-313.

886 **Krainer K, Lucas SG, Ronchi A. 2012.** Tetrapod footprints from the Alpine Buntsandstein  
887 (Lower Triassic) of the Drau Range (Eastern Alps, Austria). *Jahrbuch der Geologischen  
888 Bundesanstalt* **152**:205-212.

889 **Krebs B. 1965.** Die Triasfauna der Tessiner Kalkalpen, XIX. *Ticinosuchus ferox* nov. gen. nov.  
890 sp. *Schweizerische Paläontologische Abhandlungen* **81**:1-140.

891 **Kubo T, Benton MJ. 2007.** Evolution of hindlimb posture in archosaurs: limb stresses in extinct  
892 vertebrates. *Palaeontology* **50**(6):1519-1529.

893 **Kubo T, Benton MJ. 2009.** Tetrapod postural shift estimated from Permian and Triassic  
894 trackways. *Palaeontology* **52**(5):1029-1037.

895 **Lautenschlager S, Desojo JB. 2011.** Reassessment of the Middle Triassic rauisuchian  
896 archosaurs *Ticinosuchus ferox* and *Stagonosuchus nyassicus*. *Paläontologische Zeitschrift*  
897 **85**(4): 357-381.

898 **Leonardi G. 1987.** Glossary and manual of tetrapod footprint palaeoichnology. p.p. 117.  
899 Brasilia: Ministerio das Minas e Energia Departamento Nacional da Producao Mineral.

900 **Lorenzoni S, Zanettin E. 1958.** Contributo alla conoscenza del giacimento uranifero di Preit  
901 (Alpi Cozie). *Studi e Ricerche Divisione Geomineraria CNRN* **1**(2):349-433.

902 **Lualdi A, Bianchi U. 1990.** La Formazione di Costa Losera: una nuova unità stratigrafica  
903 dell'Anisico delle Alpi Liguri. *Atti Ticinensi di Scienze della Terra* **33**:33-62.

904 **Lualdi A, Seno S. 1984.** Osservazioni stratigrafiche e tettoniche nella zona del Rio di Nava  
905 (Brianzinese Ligure Esterno, Unità di Ormea). *Memorie della Società Geologica Italiana*  
906 **28**:493-503.

907 **Malaroda R. 1970.** Carta geologica del Massiccio dell'Argentera alla scala 1: 50.000. Allegato  
908 al vol. **9** delle *Memorie della Società Geologica Italiana*.

909 **Mallison H, Wings O. 2014.** Photogrammetry in paleontology—a practical guide. *Journal of*  
910 *Paleontological Techniques* **12**:1-31.

911 **Manning PL. 2004.** A new approach to the analysis and interpretation of tracks: examples from  
912 the dinosauria. *Geological Society, London, Special Publications*, **228(1)**: 93-123.

913 **Megard-Galli J, Baud A. 1977.** Le Trias moyen et supérieur des Alpes nord-occidentales et  
914 occidentales: données nouvelles et corrélations stratigraphiques. *Bulletin B.R.G.M.* **4(3)**:233-  
915 250.

916 **Melchor RN, De Valais S. 2006.** A review of Triassic tetrapod track assemblages from  
917 Argentina. *Palaeontology* **49(2)**:355-379.

918 **Motani R, Jiang DY, Chen GB, Tintori A, Rieppel O, Ji C, Huang JD. 2015a.** A basal  
919 ichthyosauriform with a short snout from the Lower Triassic of China. *Nature* **517(7535)**:485-  
920 488.

921 **Motani R, Jiang DY, Tintori A, Rieppel O, Chen GB, You H. 2015b.** Status of *Chaohusaurus*  
922 *chaoxianensis* (Chen, 1985). *Journal of Vertebrate Paleontology* **35(1)**:e892011.

923 **Nesbitt SJ. 2011.** The early evolution of archosaurs: relationships and the origin of major clades.  
924 *Bulletin of the American Museum of Natural History* **41(supp.)**:1-292.

925 **Nesbitt SJ, Liu J, Li C. 2010.** A sail-backed suchian from the Heshanggou Formation (Early  
926 Triassic: Olenekian) of China. *Earth and Environmental Science Transactions of the Royal*  
927 *Society of Edinburgh* **101**:271–284.

928 **Olsen PE. 1995.** A new approach for recognizing track makers. *Geological Society of America,*  
929 *Abstracts with Programs* **27**:72.

930 **Olsen PE, Smith JB, McDonald NG. 1998.** Typematerial of the type species of the classic  
931 theropod footprint genera Eubrontes, Anchisauripus and Grallator (Early Jurassic, Hartford  
932 and Deerfield basins, Connecticut and Massachusetts, U.S.A.). *J. Vertebr. Paleontol.* **18**: 586–  
933 601.

934 **Payne JL, Lehrmann DJ, Wei J, Orchard MJ, Schrag DP, Knoll AH. 2004.** Large  
935 perturbations of the carbon cycle during recovery from the end-Permian extinction. *Science*  
936 **305**:506-509.

937 **Payne JL, Summers M, Rego BL, Altiner D, Wei J, Yu M, Lehrmann DJ. 2011.** Early and  
938 Middle Triassic trends in diversity, evenness, and size of foraminifers on a carbonate platform  
939 in south China: implications for tempo and mode of biotic recovery from the end-Permian  
940 mass extinction. *Paleobiology* **37**:409-425.

941 **Peabody FE. 1948.** Reptile and amphibian trackways from the Lower Triassic Moenkopi  
942 formation of Arizona and Utah. *Bulletin of the Department of Geological sciences* **27**:295-  
943 468.

944 **Peecook BR, Smith RM, Sidor CA. 2018.** A novel archosauromorph from Antarctica and an  
945 updated review of a high-latitude vertebrate assemblage in the wake of the end-Permian mass  
946 extinction. *Journal of Vertebrate Paleontology* **38**(6):e1536664.

947 **Petti FM, Avanzini M, Belvedere M, De Gasperi M, Ferretti P, Girardi S, Remondino F,**  
948 **Tomasoni R. 2008.** Digital 3D modelling of dinosaur footprints by photogrammetry and laser  
949 scanning techniques: integrated approach at the Coste dell'Anglone tracksite (Lower Jurassic,  
950 Southern Alps, Northern Italy). *Studi Trentini di Scienze Naturali, Acta Geologica* **83**:303-  
951 315.

952 **Petti FM, Bernardi M, Kustatscher E, Renesto S, Avanzini M. 2013.** Diversity of continental  
953 tetrapods and plants in the Triassic of the Southern Alps: Ichnological, paleozoological and  
954 paleobotanical evidence. In Tanner, L.H., Spielmann, J.A. and Lucas, S.G. (eds.), The  
955 Triassic System. *New Mexico Museum of Natural History and Science, Bulletin* **61**:458-484.

956 **Peyer K, Carter JG, Sues H-D, Novak SE, Olsen PE. 2008.** A new suchian archosaur from the  
957 Upper Triassic of North Carolina. *Journal of Vertebrate Paleontology* **28**:363-381.

958 **Pough FH, Heiser JB, McFarland WN. 1996.** Vertebrate Life. Prentice Hall International, New  
959 Jersey.

960 **Racki G. 2003.** End-Permian mass extinction: oceanographic consequences of double  
961 catastrophic volcanism. *Lethaia* **35**:171-173.

962 **Racki G, Wignall PB. 2005.** Late Permian double-phased mass extinction and volcanism: an  
963 oceanographic perspective. In: Over, D.J., Morrow, J.R., Wignall, P.B. (Eds.), Understanding  
964 Late Devonian and Permian-Triassic Biotic and Climatic Events: Towards an Integrated  
965 Approach. Elsevier B.V., pp. 263-297.

966 **Remondino F, Rizzi A, Girardi S, Petti FM, Avanzini M. 2010.** 3D Ichnology—recovering  
967 digital 3D models of dinosaur footprints. *The Photogrammetric Record* **25**(131):266-282.

968 **Retallack GJ. 2005.** Permian greenhouse crises. The nonmarine Permian. *New Mexico Museum*  
969 *of Natural History and Science Bulletin* **30**:256-269.

970 **Retallack GJ.** 2009. Greenhouse crises of the past 300 million years. *Geological Society of*  
971 *America Bulletin* **121**(9-10):1441-1455.

972 **Retallack GJ.** 2013. Permian and Triassic greenhouse crises. *Gondwana Research* **24**(1):90-103.

973 **Retallack GJ, Jahren AH.** 2008. Methane release from igneous intrusion of coal during Late  
974 Permian extinction events. *The Journal of Geology* **116**:1–20.

975 **Retallack GJ, Sheldon ND, Carr PF, Fanning M, Thompson CA, Williams ML, ... Hutton**  
976 **A.** 2011. Multiple Early Triassic greenhouse crises impeded recovery from Late Permian  
977 mass extinction. *Palaeogeography, Palaeoclimatology, Palaeoecology* **308**(1-2):233–251.

978 **Romano M, Citton P, Nicosia U.** 2015. Corroborating trackmaker identification through  
979 footprint functional analysis: the case study of *Ichnitherium* and *Dimetropus*. *Lethaia*  
980 **49**:102-116.

981 **Romer AS.** 1971. The Chanares (Argentina) Triassic reptile fauna XI. Two new long-snouted  
982 thecodonts, *Chanaresuchus* and *Gualosuchus*. *Breviora* **379**:1-22.

983 **Santi G, Lualdi A, Decarlis A, Nicosia U, Ronchi A.** 2015. Chirotheriid footprints from the  
984 Lower-Middle Triassic of the Briançonnais Domain (Pelite di Case Valmarenca, Western  
985 Liguria, NW Italy). *Bollettino della Società Paleontologica Italiana* **54**(2):82.

986 **Scheyer TM, Romano C, Jenks J, Bucher H.** 2014. Early Triassic marine biotic recovery: the  
987 predators' perspective. *PLoS ONE* **9**:e88987.

988 **Septon MA, Looy CV, Brinkhuis H, Wignall PB, de Leeuw JW, Visscher H.** 2005.  
989 Catastrophic soil erosion during the end-Permian biotic crisis. *Geology* **33**:941–944.

990 **Sereno PC.** 1991. Basal archosaurs: phylogenetic relationship and functional implications.  
991 *Journal of Vertebrate Paleontology* **11**:1–53.

992 **Shen J, Chen J, Algeo TJ, Yuan S, Feng Q, Yu J, ... Planavsky NJ. 2019.** Evidence for a  
993 prolonged Permian–Triassic extinction interval from global marine mercury records. *Nature*  
994 *communications* **10**(1):1563.

995 **Schmid SM, Fügenschuh B, Kissling E, Schuster R. 2004.** Tectonic map and overall  
996 architecture of the Alpine orogen. *Eclogae Geologicae Helvetiae* **97**:93–117.

997 **Schmid SM, Kissling E, Diehl T, van Hinsbergen DJJ, Molli G. 2017.** Ivrea mantle wedge,  
998 arc of the Western Alps, and kinematic evolution of the Alps - Apennines orogenic system.  
999 *Swiss Journal of Geosciences* **110**:581–612.

1000 **Schobben M, Joachimski MM, Korn D, Leda L, Korte C. 2014.** Palaeotethys seawater  
1001 temperature rise and an intensified hydrological cycle following the end–Permian mass  
1002 extinction. *Gondwana Research* **26**:675–683.

1003 **Sepkoski JJ Jr. 1984.** A kinetic model of Phanerozoic taxonomic diversity. III. Post–Paleozoic  
1004 families and mass extinctions. *Paleobiology* **10**:246–267.

1005 **Smith RMH, Evans SE. 1996.** New material of *Youngina*: evidence of juvenile aggregation in  
1006 Permian diapsid reptiles. *Palaeontology* **39**:289–303.

1007 **Song H, Wignall PB, Tong J, Yin H. 2013.** Two pulses of extinction during the Permian–  
1008 Triassic crisis. *Nature Geoscience* **6**(1):52.

1009 **Song H, Wignall PB, Tong J, Song H, Chen J, Chu D, ... Lai X. 2015.** Integrated Sr isotope  
1010 variations and global environmental changes through the Late Permian to early Late Triassic.  
1011 *Earth and Planetary Science Letters* **424**:140–147.

1012 **Sookias RB, Butler RJ. 2013.** Euparkeriidae. *Geological Society, London, Special Publications*  
1013 **379**:35–48.

1014 **Sues HD, Desojo JB, Ezcurra MD. 2013.** Doswelliidae: a clade of unusual armoured

1015 archosauriforms from the Middle and Late Triassic. *Geological Society, London, Special*  
1016 *Publications* **379**:SP379-13.

1017 **Sun Y, Joachimski M, Wignall PB, Yan C, Chen Y, Jiang H, Wang L, Lai X. 2012.** Lethally  
1018 Hot Temperatures During the Early Triassic Greenhouse. *Science* **338**:1-35.

1019 **Torsvik TH, Van Der Voo R, Preeden U, Mac C, Steinberger B, Doubrovine PV, van**  
1020 **Hinsbergen DJJ, Domeier M, Gaina C, Tohver E, Meert JG, McCausland PJA, Cocks**  
1021 **LRM. 2012.** Earth-Science Reviews Phanerozoic polar wander, palaeogeography and  
1022 dynamics. *Earth Science Reviews* **114**(3-4):325-368.

1023 **Treasise G, Sarjeant WAS. 1997.** The tracks of Triassic Vertebrates. Fossil Evidence from  
1024 North-West England. The stationery Office, London, 204 pp.

1025 **Trotteyn MJ, Arcucci AB, Raugust T. 2013.** Proterochampsia: an endemic archosauriform  
1026 clade from South America. In: Anatomy, Phylogeny and Palaeobiology of Early Archosaurs  
1027 and their Kin (eds Nesbitt S.J., Desojo J.B., Irmis R.B.), *Geological Society, London, Special*  
1028 *Publications* **379**:59-90.

1029 **Van Hinsbergen DJJ, De Groot LV, Van Schaik SJ, Spakman W, Bijl PK, Sluijs A,**  
1030 **Langereis CG, Brinkhuis H. 2015.** A paleolatitude calculator for paleoclimate studies. *PLoS*  
1031 *ONE* **10**(6):1-21.

1032 **Vanossi M. 1969.** La serie brianzone di Salto del Lupo (Liguria Occ.): osservazioni  
1033 sedimentologico-stratigrafiche. *Atti Ist. Geol. Univ. Pavia* **20**: 3-16.

1034 **Vanossi M. 1974.** L'Unità di Ormea: una chiave per l'interpretazione del Brianzone ligure.  
1035 Tipografia del libro.

1036 **Vanossi M. 1991.** Guide Geologiche Regionali, 11 itinerari, Alpi Liguri (a cura della SGI), 296  
1037 pp. BE-MA Edit., Milano.

1038    **Welles SP. 1947.** Vertebrates from the Upper Moenkopi Formation of Northern Arizona.

1039         *University of California Publications in Geological Science* **27**:241-294.

1040    **Whiteside JH, Ward PD. 2011.** Ammonoid diversity and disparity track episodes of chaotic

1041         carbon cycling during the early Mesozoic. *Geology* **39**:99–102.

1042    **Wignall PR. 2001.** Large igneous provinces and mass extinctions. *Earth-Science Reviews* **53**:1–

1043         33.

1044    **Wilson JA 2005.** Integrating ichnofossil and body fossil records to estimate locomotor posture

1045         and spatiotemporal distribution of early sauropod dinosaurs: a stratocladistic approach.

1046         *Paleobiology* **31**(3): 400-423.

1047    **Withers PC. 1992.** Comparative Animal Physiology. Saunders College, New York.

1048    **Xing LD, Klein H, Lockley MG, Li J, Zhang J, Matsukawa M, Xiao J. 2013.** *Chirotherium*

1049         trackways from the Middle Triassic of Guizhou, China. *Ichnos* **20**:99–107.

1050    **Young CC. 1964.** The pseudosuchians in China. *Palaeontologia Sinica Series C* **19**:105-205.

1051    **Zhang F. 1975.** A new thecodont *Lotosaurus*, from Middle Triassic of Hunan. *Vertebrata*

1052         *PalAsiatica* **13**:144-147.

1053    **Ziegler PA, Stampfli GM. 2001.** Late Palaeozoic–Early Mesozoic plate boundary

1054         reorganization: collapse of the Variscan orogen and opening of Neotethys. In: Cassinis G.

1055         (Ed.), Permian Continental Deposits of Europe and Other Areas. Regional Reports and

1056         Correlations. *Annali Museo Civico Scienze Naturali, Brescia* **25**:17–34.

1057

1058    **Figure captions**

1059

1060 **Fig. 1** - Geologic map of the Pianezza area. In the upper row the location of Maira Valley and  
1061 Gardetta-Pianezza area. For the geologic map: 1= volcanic complex and graphitic schist  
1062 (upper Carboniferous - Permian); 2= conglomerate, 3= quartz-conglomerate, and 4= quartz-  
1063 arenite and quartz-siltite of the quartzitic complex (upper Permian - early Lower Triassic); 5=   
1064 lower carniole complex (late Lower Triassic); 6= lower calcareous complex (lower Anisian -  
1065 early upper Ladinian); 7= upper dolomitic complex (upper Ladinian); 8= lakes and peat bog;  
1066 9= faults; 10= location of the footprint site; in white the detritic cover and moraines.

1067 **Fig. 2** - Correlation scheme among the Briançonnais s.s., the Ligurian Briançonnais, from De  
1068 Carlis & Lualdi, 1990 redrawn and modified. PNQ: “Ponte di Nava Quartzites”, CVP: Case  
1069 Val Marenca Pelites. The footprint silhouette marks the position of the track-bearing horizon.

1070 **Fig. 3** – a) Panoramic view of the track surface with the line-drawing of the chirotherian  
1071 trackways. In pale yellow the above-lying bed characterized by symmetric wave ripples; b)  
1072 Detailed view of the GT-1 and GT-2 trackways, highlighted with the black colour.

1073 **Fig. 4** – *Isochirotherium gardettae* ichnosp. nov. The GT-7 trackway, made of three consecutive  
1074 manus-pes couples, is here highlighted by the red chalk and preserved in the upper track-  
1075 bearing surface. Scale bar: 13 cm.

1076 **Fig. 5** – a) *Isochirotherium gardettae* ichnosp. nov. Colour-coded and contour line image of the  
1077 GT-7 trackway; b) Interpretative drawing of the GT-7 trackway.

1078 **Fig. 6** – Reconstruction of the trackmaker’s fore- and hind limbs, based on the 3D model and its  
1079 interpretative drawing. Dashed lines define the metatarsal of digit V held lifted off the ground  
1080 during locomotion.

1081 **Fig. 7** – Pentadactyl tracks from the Lower and Middle Triassic, assigned to the ichnogenus  
1082 *Chirotherium* and their comparison with the studied tracks of the Gardetta ichnosite: a) GT-1-  
1083 3; b) GT-2-3; c) GT-2-8; d) GT-2-6; e), f) *Chirotherium barthii* pes manus sets from type  
1084 surface of the “Thüringischer Chirotheriensandstein”, Hildburghausen, Germany; g)  
1085 *Chirotherium barthii* pes manus set from the Holbrook Member of the Moenkopi Formation  
1086 (Middle Triassic), southwest of Cameron, northern Arizona; h) *Chirotherium vorbachi* pes  
1087 manus set from the Lower Triassic of Aura an der Saale, Germany; i), *Chirotherium sickleri*  
1088 “Thüringischer Chirotheriensandstein”, Germany; l), m) *Chirotherium sickleri* pes manus  
1089 sets from the Wupatki Member of the Moenkopi Formation (Lower Triassic), Meteor Crater,  
1090 Arizona. Scale bar 10 cm.

1091 **Fig. 8** - Pentadactyl tracks from the Lower and Middle Triassic, assigned to the ichnogenus  
1092 *Isochirotherium* and their comparison with the studied tracks of the Gardetta ichnosite: a), b),  
1093 c), pes manus sets of the GT-7 trackway; d) GT-3 isolated pes imprints of the lower track  
1094 surface; e) *Isochirotherium herculis* pes manus set from the “Thüringischer  
1095 Chirotheriensandstein” (Lower Triassic), Germany; f) *Isochirotherium marshalli* pes manus  
1096 set from the Holbrook Member of the Moenkopi Formation (Middle Triassic), Penzance,  
1097 Northern Arizona; g) *Isochirotherium inferni* manus pes set from the Middle Triassic (late  
1098 Anisian) of Adige Valley, Bolzano, Italy; h) *Isochirotherium coltoni* pes manus set from the  
1099 Wupatki Member of the Moenkopi Formation (Lower Triassic), Meteor Crater, Arizona; i)  
1100 *Isochirotherium lomasi* pes manus set from the Middle Triassic (Anisian) of Cheshire, Great  
1101 Britain; l) *Isochirotherium coureli* pes manus set from the Middle Triassic (Anisian-Ladinian)  
1102 of the Massif Central, France; m) *Isochirotherium hessbergense* pes manus set from the  
1103 “Thüringischer Chirotheriensandstein” (Lower Triassic), Germany; n) *Isochirotherium*

1104 *demathieu* pes manus set from the Middle Triassic of Mont d'Or Lyonnais, France; o)

1105 *Isochirotherium soergeli* pes manus set from the “Thüringischer Chirotheriensandstein”

1106 (Lower Triassic), Germany. Scale bar 10 cm.

1107 **Fig. 9** – Fore- and hind-limb skeletons of Triassic archosauriforms and of the *Isochirotherium*  
1108 *gardettae* trackmaker. Reconstructed right pes and manus skeletons of a) the *Isochirotherium*  
1109 *gardettae* trackmaker in anterior/dorsal view; b) *Postosuchus kirkpatricki* CHATTERJEE 1985,  
1110 USA, Norian; c) *Postosuchus alisonae*, PEYER et al. 2008, USA, Norian; d) *Lotosaurus*  
1111 *adentus* ZHANG, 1975, China, Ladinian; e) *Proterosuchus fergusi* BROOM 1903, South Africa,  
1112 Induan–?early Olenekian f) *Erythrosuchus africanus* BROOM 1905, South Africa, early  
1113 Anisian; g) *Shansisuchus shansisuchus* YOUNG 1964, China, late Anisian; h) *Euparkeria*  
1114 *capensis* Broom, 1913, South Africa, Anisian; i) *Chanaresuchus bonapartei* ROMER, 1971,  
1115 Argentina, Ladinian. Scale bars: a), b), c), d), f) g) = 10 cm; e), h) and i) = 1 cm.

1116 **Fig. 10** – Life appearance of the non-archosaurian archosauriform (?Erythrosuchid) the most  
1117 suitable producer of *Isochirotherium gardettae*. Simplified reconstruction of fore and hind  
1118 autopodials in bottom (a) view. Complete life reconstruction in bottom (b), back (c), frontal  
1119 (d) and lateral view (e) of the trackmaker. The gait and fore- and hind limbs were  
1120 reconstructed according to the pattern and morphologies of GT-7 trackway (artwork by the  
1121 Italian artist Fabio Manucci). See the supplementary video to get a more complete view of the  
1122 reconstruction.

1123 **Fig. 11** – Paleogeographic distribution of Early Triassic archosauriform footprints (yellow stars)  
1124 and body fossil localities across Pangea. Black square = indeterminate archosauromorphs, red  
1125 circles = non-archosauriform archosauromorphs, blue stars = archosauriforms. The  
1126 palaeolatitude estimate for the southern Briançonnais domain is 11.8 N in the Olenekian (250

1127 Ma), confirming that archosauriforms were distributed also at low latitudes, in the tropical  
1128 humid climatic belt. ImagePaleomap for 250 Ma downloaded from Fossilworks using data  
1129 from the Paleobiology Database (Alroy, 2003). Redrawn and modified from Bernardi et al.,  
1130 2015 and Benton (2018).

1131

# Figure 1

Geologic map of the Pianezza area

**Fig. 1** - Geologic map of the Pianezza area. In the upper row the location of Maira Valley and Gardetta-Pianezza area. For the geologic map: (1) volcanic complex and graphitic schist (upper Carboniferous - Permian). (2) Conglomerate. (4) Quartz-conglomerate, and quartz-arenite and quartz-siltite of the quartzitic complex (upper Permian - early Lower Triassic). (5) Lower carniole complex (late Lower Triassic). (6) Lower calcareous complex (lower Anisian - early upper Ladinian). (7) Upper dolomitic complex (upper Ladinian). (8) Lakes and peat bog. (9) Faults. (10) Location of the footprint site. In white the detritic cover and moraines.

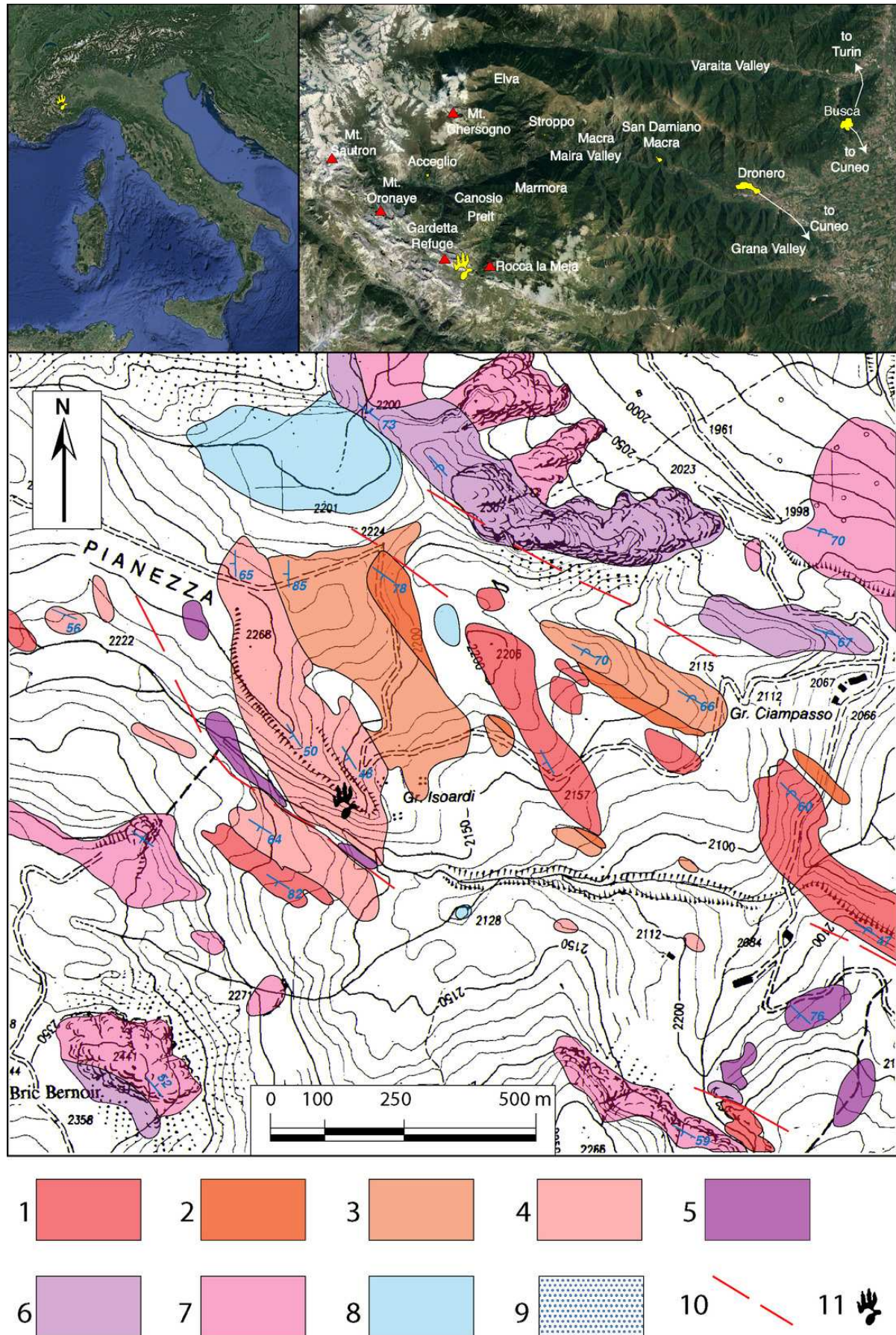


## Figure 2

Correlation scheme among the Briançonnais s.s., the Ligurian Briançonnais

**Fig. 2** - Correlation scheme among the Briançonnais s.s., the Ligurian Briançonnais, from De Carlis & Lualdi, 1990 redrawn and modified. (PNQ) “Ponte di Nava Quartzites”. (CVP) Case Val Marenca Pelites. The footprint silhouette marks the position of the track-bearing horizon.

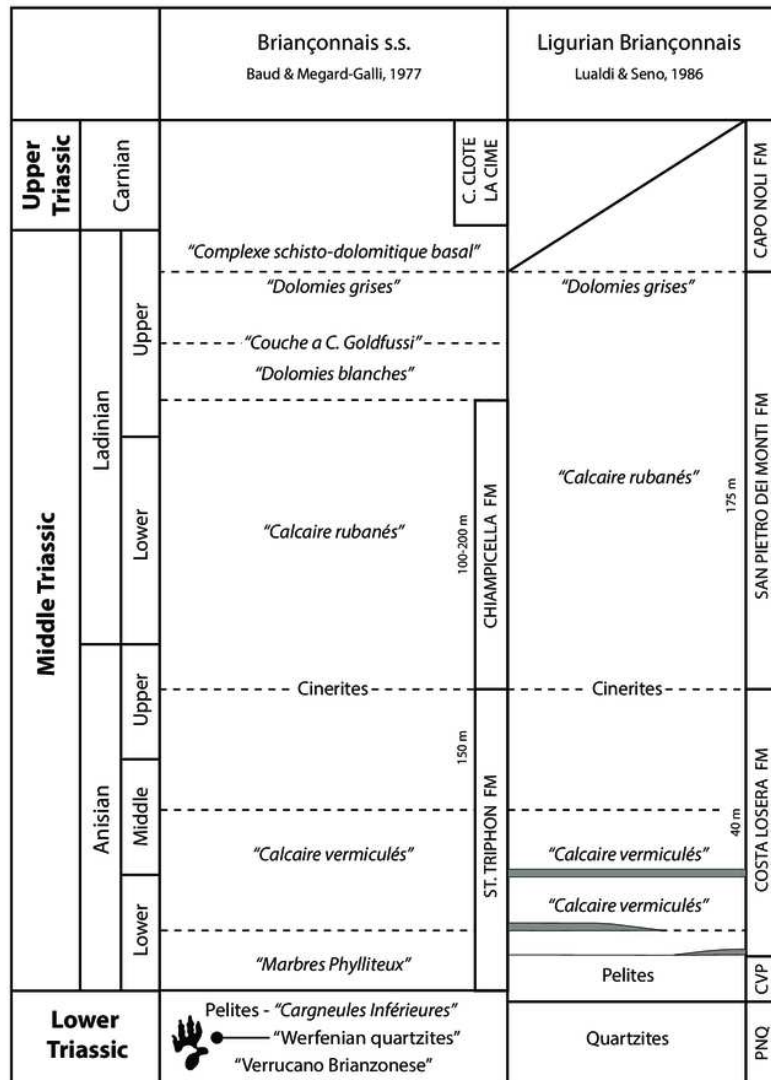


## Figure 3

Panoramic view of the track surface with the line-drawing of the chirotherian trackways

**Fig. 3** - (a) Panoramic view of the track surface with the line-drawing of the chirotherian trackways. In pale yellow the above-lying bed characterized by symmetric wave ripples. (b) Detailed view of the GT-1 and GT-2 trackways, highlighted with the black colour.

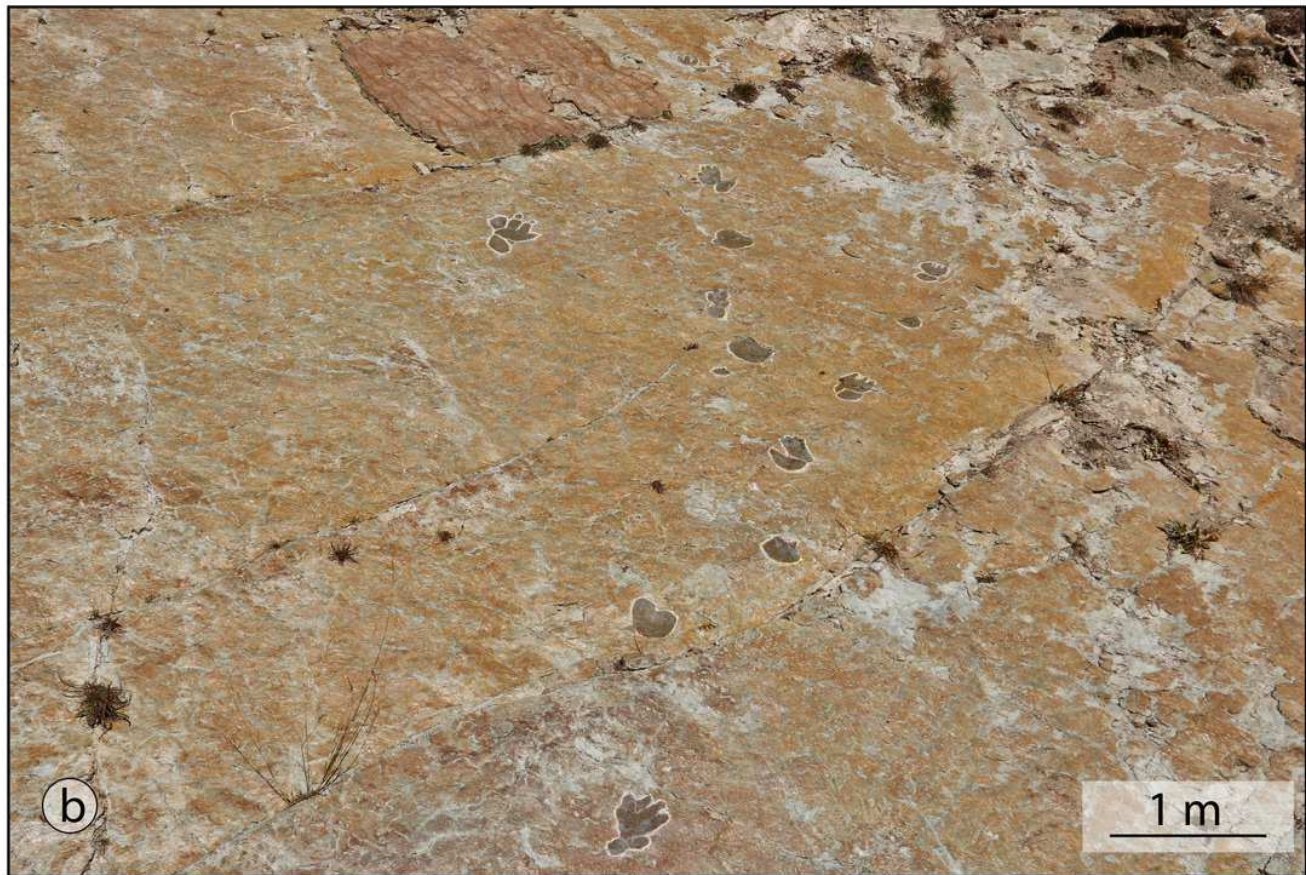
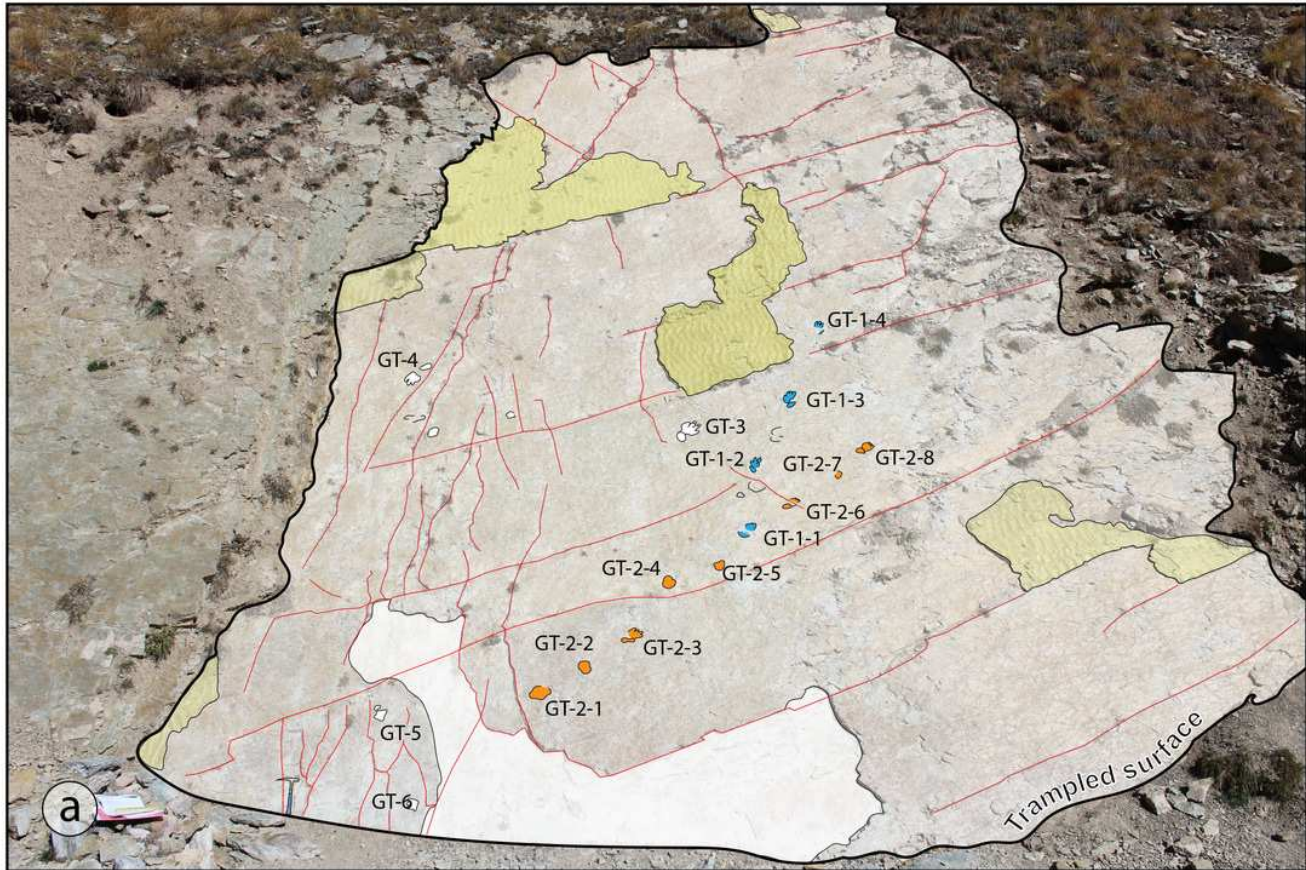


## Figure 4

*Isochirotherium gardettæ* ichnosp. nov

**Fig. 4** - *Isochirotherium gardettæ* ichnosp. nov. The GT-7 trackway, made of three consecutive manus-pes couples, is here highlighted by the red chalk and preserved in the upper track-bearing surface. Scale bar: 13 cm.



## Figure 5

*Isochirotherium gardettae* ichnosp. nov. Colour-coded and contour line image of the GT-7 trackway

**Fig. 5** - a) *Isochirotherium gardettae* ichnosp. nov. Colour-coded and contour line image of the GT-7 trackway; b) Interpretative drawing of the GT-7 trackway.

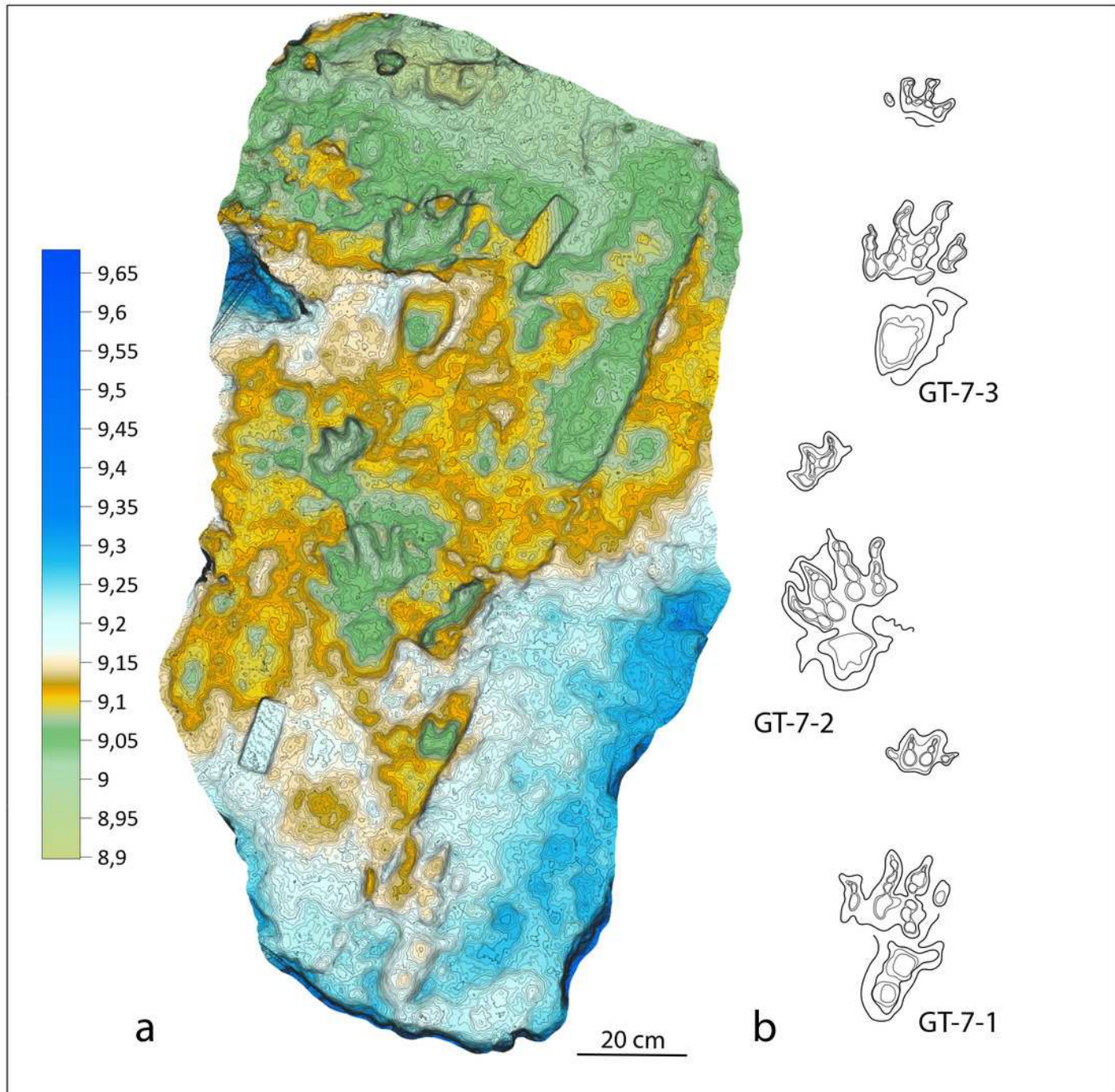


## Figure 6

Reconstruction of the trackmaker's fore- and hind limbs, based on the 3D model and its interpretative drawing

**Fig. 6** – Reconstruction of the trackmaker's fore- and hind limbs, based on the 3D model and its interpretative drawing. Dashed lines define the metatarsal of digit V held lifted off the ground during locomotion.

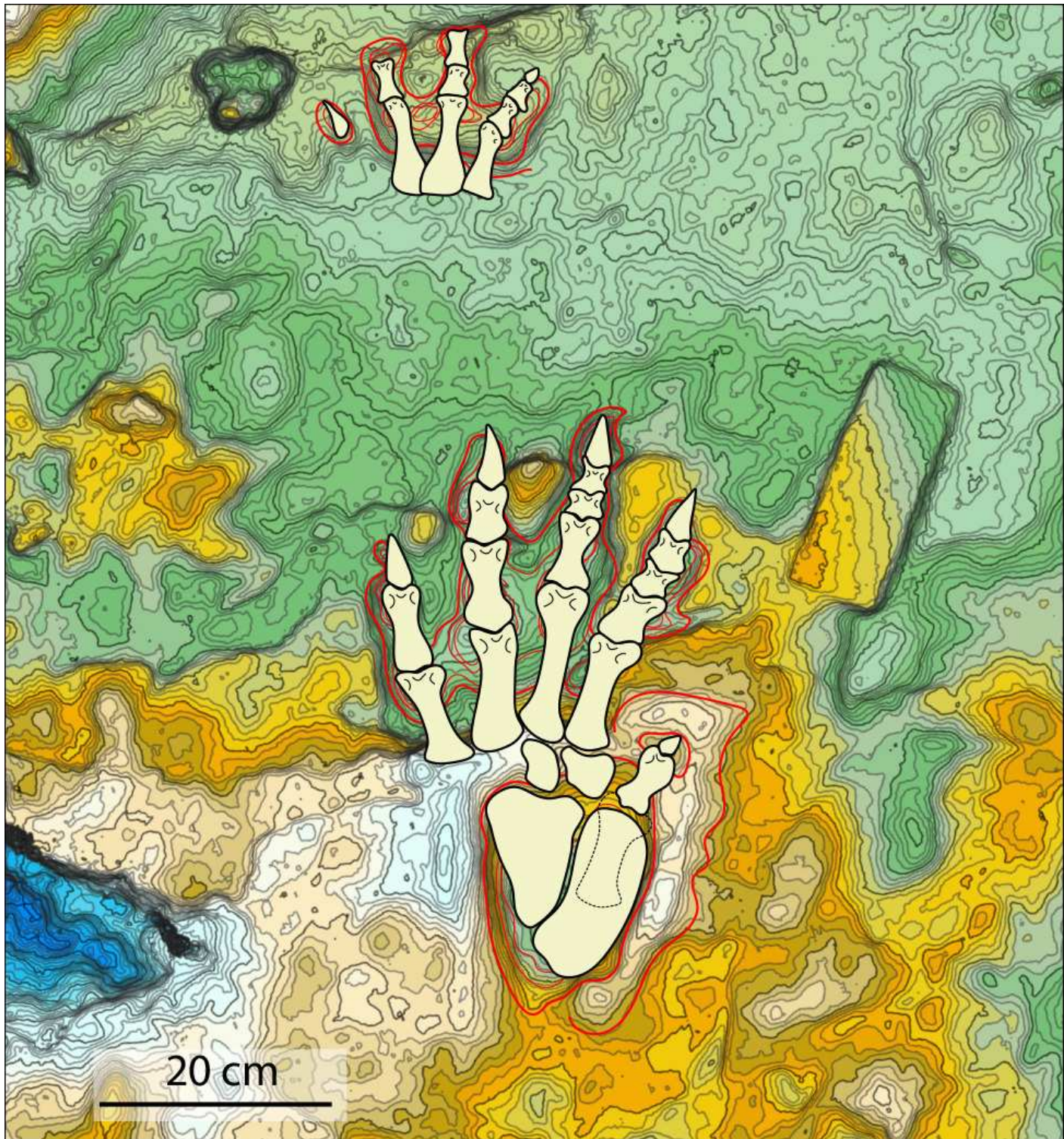


## Figure 7

Pentadactyl tracks from the Lower and Middle Triassic, assigned to the ichnogenus *Chirotherium* and their comparison with the studied tracks of the Gardetta ichnosite

**Fig. 7** – Pentadactyl tracks from the Lower and Middle Triassic, assigned to the ichnogenus *Chirotherium* and their comparison with the studied tracks of the Gardetta ichnosite. (a) GT-1-3. (b) GT-2-3. (c) GT-2-8. d) GT-2-6; (e) and (f) *Chirotherium barthii* pes manus sets from type surface of the “Thüringischer Chirotheriensandstein”, Hildburghausen, Germany. (g) *Chirotherium barthii* pes manus set from the Holbrook Member of the Moenkopi Formation (Middle Triassic), southwest of Cameron, northern Arizona. (h) *Chirotherium vorbachi* pes manus set from the Lower Triassic of Aura an der Saale, Germany (i), *Chirotherium sickleri* “Thüringischer Chirotheriensandstein”, Germany. (l) and (m) *Chirotherium sickleri* pes manus sets from the Wupatki Member of the Moenkopi Formation (Lower Triassic), Meteor Crater, Arizona. Scale bar 10 cm.

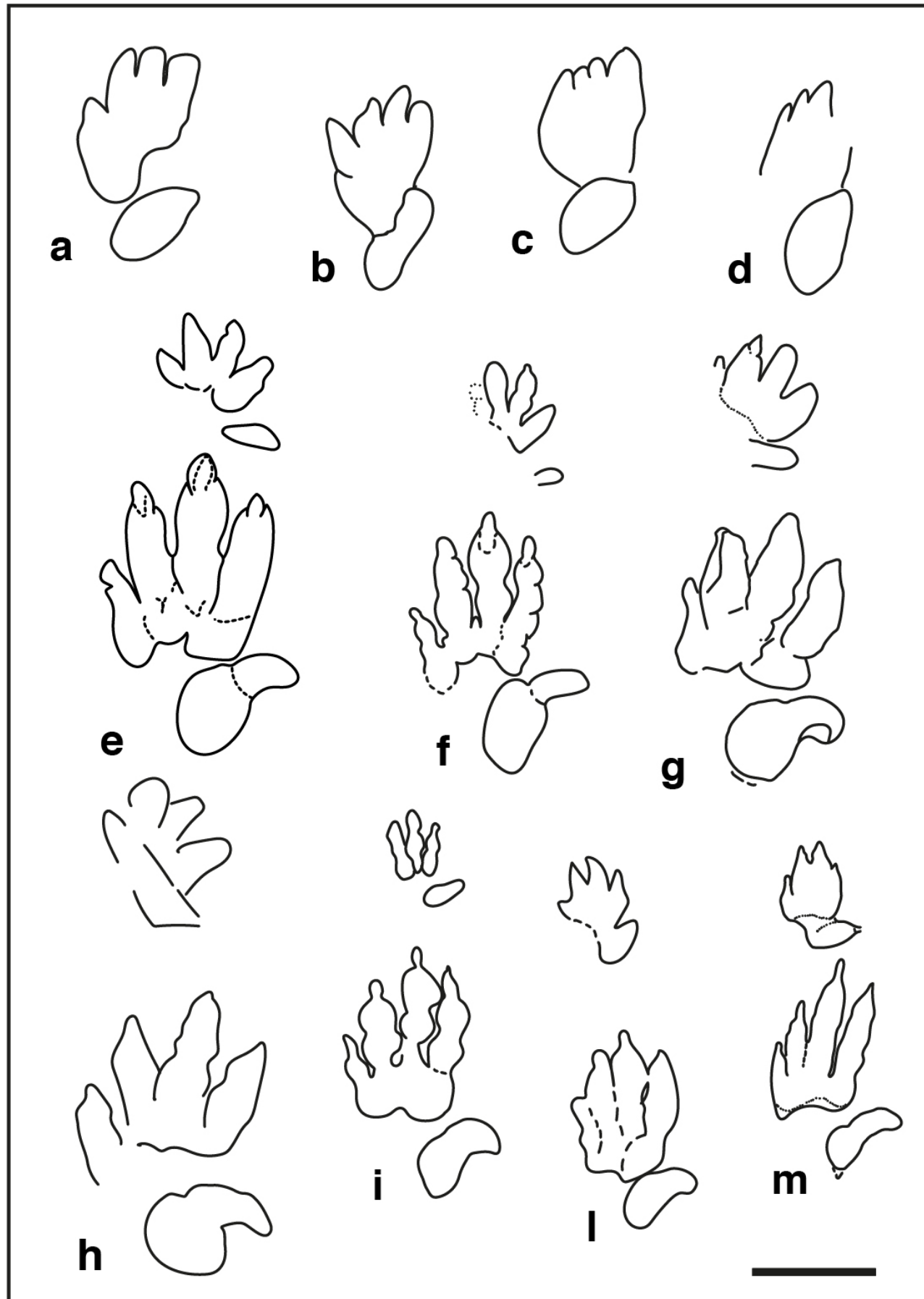


## Figure 8

Pentadactyl tracks from the Lower and Middle Triassic, assigned to the ichnogenus *Isochirotherium* and their comparison with the studied tracks of the Gardetta ichnosite

**Fig. 8** - Pentadactyl tracks from the Lower and Middle Triassic, assigned to the ichnogenus *Isochirotherium* and their comparison with the studied tracks of the Gardetta ichnosite (a), (b), (c) Pes manus sets of the GT-7 trackway. (d) GT-3 isolated pes imprints of the lower track surface. (e) *Isochirotherium herculis* pes manus set from the “Thüringischer Chirotheriensandstein” (Lower Triassic), Germany. (f) *Isochirotherium marshalli* pes manus set from the Holbrook Member of the Moenkopi Formation (Middle Triassic), Penzance, Northern Arizona. (g) *Isochirotherium inferni* manus pes set from the Middle Triassic (late Anisian) of Adige Valley, Bolzano, Italy. (h) *Isochirotherium coltoni* pes manus set from the Wupatki Member of the Moenkopi Formation (Lower Triassic), Meteor Crater, Arizona. (i) *Isochirotherium lomasi* pes manus set from the Middle Triassic (Anisian) of Cheshire, Great Britain. (l) *Isochirotherium coureli* pes manus set from the Middle Triassic (Anisian-Ladinian) of the Massif Central, France. (m) *Isochirotherium hessbergense* pes manus set from the “Thüringischer Chirotheriensandstein” (Lower Triassic), Germany. (n) *Isochirotherium demathieui* pes manus set from the Middle Triassic of Mont d’Or Lyonnais, France. (o) *Isochirotherium soergeli* pes manus set from the “Thüringischer Chirotheriensandstein” (Lower Triassic), Germany. Scale bar 10 cm.

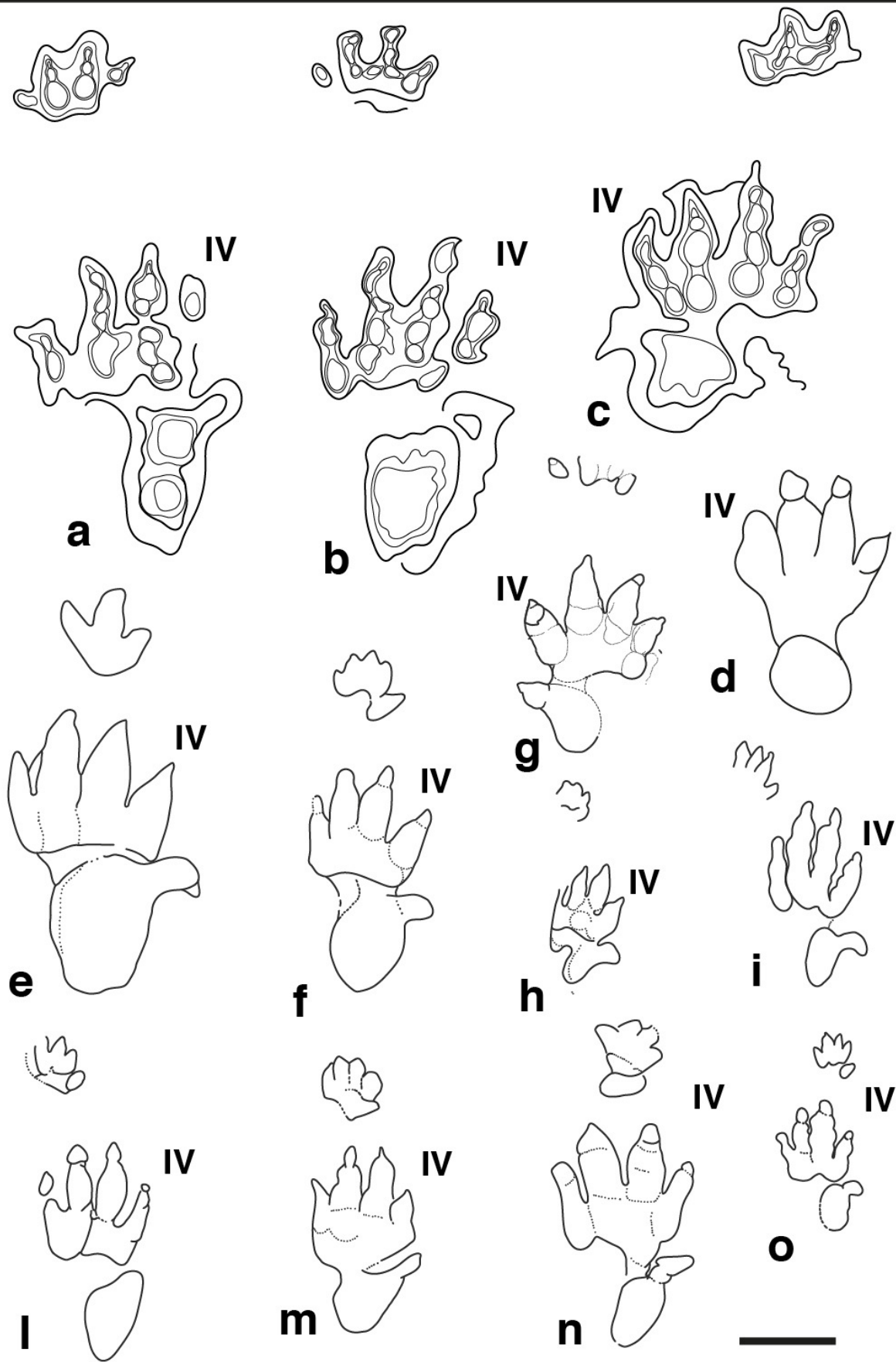


## Figure 9

Fore- and hind-limb skeletons of Triassic archosauriforms and of the *Isochirotherium gardettæ* trackmaker

**Fig. 9** – Fore- and hind-limb skeletons of Triassic archosauriforms and of the *Isochirotherium gardettæ* trackmaker. Reconstructed right pes and manus skeletons of (a) The *Isochirotherium gardettæ* trackmaker in anterior/dorsal view. (b) *Postosuchus kirkpatricki* Chatterjee 1985, USA, Norian. (c) *Postosuchus alisonae*, Peyer et al. 2008, USA, Norian. (d) *Lotosaurus adentus* Zhang, 1975, China, Ladinian. (e) *Proterosuchus fergusi* Broom 1903, South Africa, Induan-?early Olenekian. (f) *Erythrosuchus africanus* Broom 1905, South Africa, early Anisian. (g) *Shansisuchus shansisuchus* Young 1964, China, late Anisian. (h) *Euparkeria capensis* Broom, 1913, South Africa, Anisian. (i) *Chanaresuchus bonapartei* Romer, 1971, Argentina, Ladinian. Scale bars: a), b), c), d), f) g) = 10 cm; e), h) and i) = 1 cm.

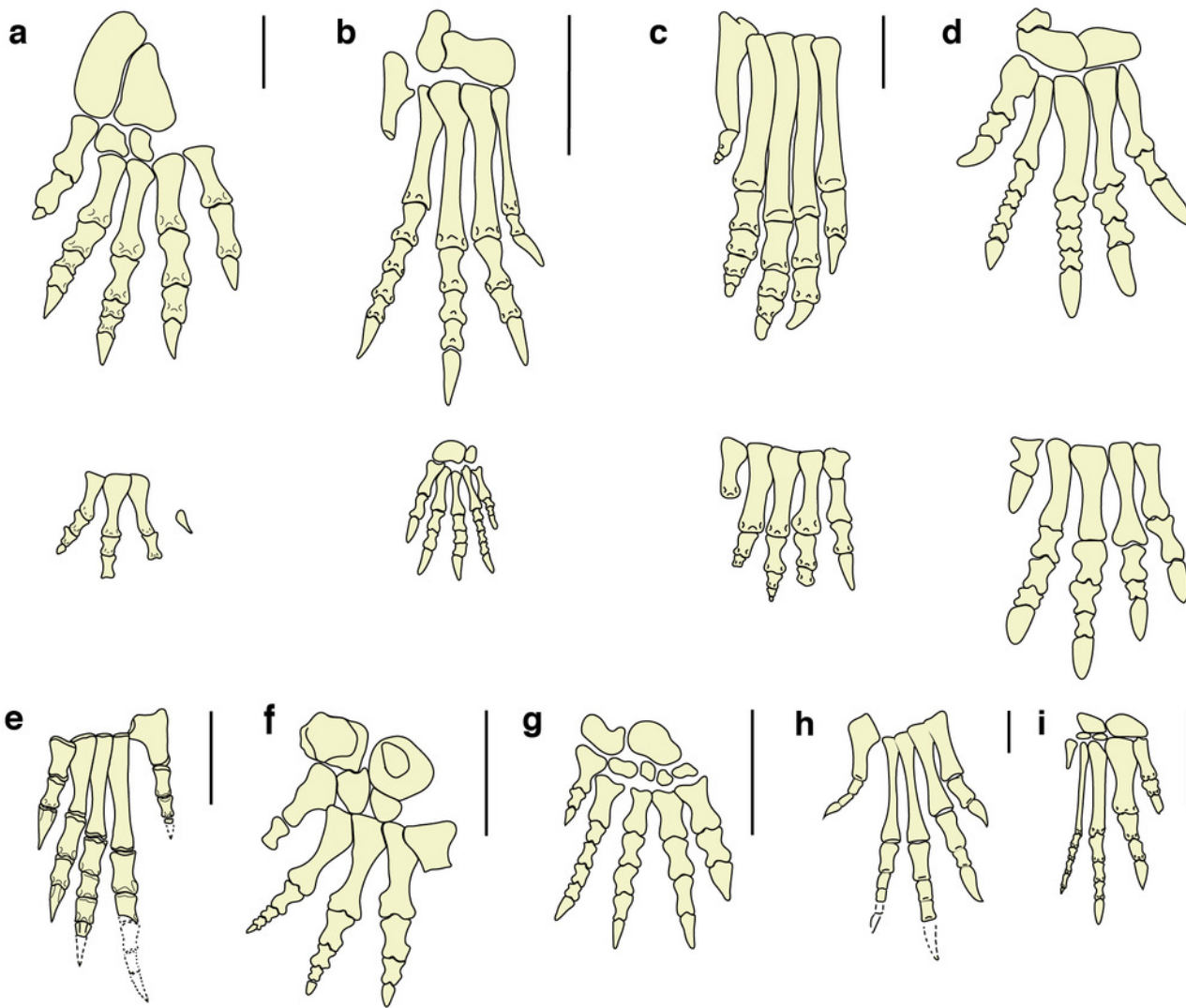


## Figure 10

Life appearance of the non-archosaurian archosauriform (?Erythrosuchid) the most suitable producer of *Isochirotherium gardettiae*

**Fig. 10** – Life appearance of the non-archosaurian archosauriform (?Erythrosuchid) the most suitable producer of *Isochirotherium gardettiae*. Simplified reconstruction of fore and hind autopodials in bottom (a) view. Complete life reconstruction in bottom (b), back (c), frontal (d) and lateral view (e) of the trackmaker. The gait and fore- and hind limbs were reconstructed according to the pattern and morphologies of GT-7 trackway (artwork by the Italian artist Fabio Manucci). See the supplementary video to get a more complete view of the reconstruction.



## Figure 11

Paleogeographic distribution of Early Triassic archosauriform footprints and body fossil localities across Pangea

**Fig. 11** – Paleogeographic distribution of Early Triassic archosauriform footprints (yellow stars) and body fossil localities across Pangea. Black square = indeterminate archosauromorphs, red circles = non-archosauriform archosauromorphs, blue stars = archosauriforms. The palaeolatitude estimate for the southern Briançonnais domain is 11.8 N in the Olenekian (250 Ma), confirming that archosauriforms were distributed also at low latitudes, in the tropical humid climatic belt. ImagePaleomap for 250 Ma downloaded from Fossilworks using data from the Paleobiology Database (Alroy, 2003). Redrawn and modified from Bernardi et al., 2015 and Benton (2018).

